LBL-13856
Preprint

Lawrence Berkeley Laboratory
UNIVERSITY OF CALIFORNIA

Physics, Computer Science & Mathematics Division

Submitted for publication

PHYSICS OF INTERMEDIATE VECTOR BOSONS

John Ellis, Mary K. Gaillard, Georges Girardi,
and Paul Sorba

January 1982

Prepared for the U.S. Department of Energy under Contract DE-AC03-76SF00098

DISCLAIMER

January 1982

LBL-13856
LAPP-TH-52

PHYSICS OF INTERMEDIATE VECTOR BOSONS*

John Ellis

CERN, Geneva, Switzerland

Mary K. Gaillard

Lawrence Berkeley Laboratory

and

Department of Physics
University of California
Berkeley, California 94720, U.S.A.

Georges Girardi

and

Paul Sorba

L.A.P.P. Annecy-le-Vieux, France

---

* This work was supported by the Director, Office of Energy Research, Office of High Energy and Nuclear Physics, Division of High Energy Physics of the U.S. Department of Energy under Contract DE-AC03-76SF00098.

I. INTRODUCTION

Since the first accelerator neutrino experiment (Danby et al 1962), searches for the vector bosons hypothesized (Fermi 1933, Yukawa 1935) as mediators of the weak interactions have been uniformly unsucessful. Nevertheless most theorists fully expect forthcoming experiments to uncover these particles, and believe that they can accurately predict their masses, decay properties and production rates. The reason for this confidence is the astonishing success of the now "standard" model (Glashow 1961, Weinberg 1967, Salam 1968) of electromagnetic and weak interactions.

The model was constructed presuming that elementary particle interactions should be describable by a "renormalizable" field theory - that is, one in which all observables are calculable in terms of a finite number of measured parameters. Quantum electrodynamics is the prototype: once the electron's mass and charge are specified, photon and electron scattering amplitudes may be calculated to any desired accuracy. Years of effort to formulate a similarly calculable weak interaction theory finally bore fruit with the work of Gerhard 't Hooft (1971) who demonstrated the renormalizability (see also Lee & Zinn Justin 1972) of a class of theories with massive, electrically charged vector bosons as required to reproduce the observed structure of Fermi weak interaction couplings. A simple example of such a theory had been written down (Glashow 1961, Weinberg 1967, Salam 1968) several years earlier, but it predicted the existance of a type of weak interaction - neutral currents - which had not been observed. Renewed interest

in the model spurred dedicated experimental searches which uncovered (Hasert et al 1973) the predicted phenomena, and, when the dust settled all the data appeared consistant with the first simple model which we describe below.

Within the present state of technology renormalizable theories must satisfy a tight set of contraints.

1) They include only fields with intrinsic angular momentum (spin) $S \leqslant 1$.

2) They include only couplings of dimension* 4 or less. Bose fields have intrinsic dimension 1 and fermions 3/2, so elementary couplings are at most trilinear in fermions and quadrilinear in bosons.

3) If spin-one (vector) fields are included, the theory must be invariant under local "gauge" transformations.

We illustrate this property of gauge invariance with a simple model, namely quantum electrodynamics, with the Lagrangian

$$\mathcal{L}_{QED} = -\frac{1}{4} F_{\mu\nu}F^{\mu\nu} + i \sum_a \bar{\psi}_a \gamma^\mu D_\mu \psi_a + \sum_a m_a \bar{\psi}_a \psi_a, \tag{1.1}$$

where A_μ is the electromagnetic field (photon) and

$$F_{\mu\nu} = \partial_\mu A_\nu - \partial_\nu A_\mu \tag{1.2}$$

is the field strength; ψ_a is a fermion field (quark or lepton) of mass m_a and charge q_a. The "covariant derivative" D_μ is related to the ordinary derivative $\partial_\mu = \frac{\partial}{\partial x^\mu}$ by

---

* In mass units. Throughout we set $\hbar = c = 1$.

$$D_\mu = \partial_\mu - ie A_\mu Q \tag{1.3}$$

where Q is the electric charge operator in units of the positron charge e:

$$Q\psi_a = q_a\psi_a. \tag{1.4}$$

It is easy to see that the Lagrangian (1.1) is invariant under local (space-time dependent) phase transformations on fermion fields

$$\psi \to e^{ie\lambda(x)Q}\psi \tag{1.5}$$

if they are accompanied by a corresponding shift (change of "gauge") in the photon field

$$A_\mu \to A_\mu + \partial_\mu\lambda(x) \tag{1.6}$$

This invariance reflects the fact that A_μ is not an observable: the observable field strength $F_{\mu\nu}$ is invariant under (1.6). Moreover gauge invariance insures the cancellation of infinities which would otherwise arise in the calculation of multiple photon exchange contributions to scattering amplitudes.

While the photon kinetic energy ($-\frac{1}{4} F_{\mu\nu}F^{\mu\nu}$) is gauge invariant, a photon mass ($\frac{m^2}{2} A_\mu A^\mu$) would not be. This was one of the stumbling blocks to the construction of a theory involving the necessarily massive vectors of the weak interactions. A second stumbling block was that they carry electric charge and therefore couple to the photon. The generalization of gauge invariance to the case of self-interacting vectors was worked out by Yang and Mills (1954), but the proof that such theories are renormalizable was complete only with the work

of 't Hooft (1971).

The Lagrangian for a general Yang-Mills theory, including fermions, can be written in the form

$$\mathcal{L}_{YM} = -\frac{1}{4} G^i_{\mu\nu} G^{\mu\nu}_i + \bar{\psi}\not{D}\psi, \quad \not{D} = D_\mu \gamma^\mu, \tag{1.7}$$

where ψ is a column matrix with elements ψ_a and the covariant derivative is now a matrix:

$$D_{\mu a}{}^b = \delta_a{}^b \partial_\mu - i V^i_\mu g_{ia}{}^b ; \tag{1.8}$$

the fermionic current $\bar{\psi}^a \gamma^\mu \psi_b$ couples to the vector V^i_μ with strength $g_{ia}{}^b$. The generalized field strength is

$$G^i_{\mu\nu} = \partial_\mu V^i_\nu - \partial_\nu V^i_\mu + c_{ijk} V^j_\mu V^k_\nu . \tag{1.9}$$

The Lagrangian (1.7) will be invariant under an infinitesinial gauge transformation ($\lambda(x) \ll 1$):

$$\begin{aligned} \delta\psi &= i\lambda^i(x) g_i \psi \\ \delta V^i_\mu &= \partial_\mu \lambda^i(x) - c_{ijk} \lambda^j(x) V^k_\mu \end{aligned} \tag{1.10}$$

if the c_{ijk} are totally antisymmetric and we impose

$$[g_i, g_j] = i c_{ijk} g_k \tag{1.11}$$

$$c_{ijk} c_{k\ell m} = c_{ikm} c_{kj\ell} + c_{i\ell k} c_{kjm} . \tag{1.12}$$

These conditions mean that the g_i represent the infinitesimal generators of a group g with structure constants c_{ijk}. The field strength $G^i_{\mu\nu}$ transforms according to the adjoint representation of g:

$$\delta G^i_{\mu\nu} = - c_{ijk} \lambda^j(x) G^k_{\mu\nu} . \tag{1.13}$$

The rules that emerge for constructing a renormalizable theory with vectors are thus:

1) The Lagrangian must be invariant under a group of local gauge transformations.

2) The spin-1 fields must transform according to the adjoint representation of g, determining uniquely their multiplicity.

3) Fermions must transform according to some (reducible) representation of g with their couplings to vectors given by representation matrices for the generators.

We did not include a fermion mass term in (1.7) because we will consider gauge transformations which depend on helicity (the spin conponent along the direction of momentum), and which are not respected by mass terms. In such theories fermions, like vectors, acquire their masses from symmetry breaking effects.

Let us recall the status of weak interactions before the discovery of neutral currents (Hasert et al 1973). Their two distinctive features where that only "left-handed" (negative helicity) fermions participated in weak couplings and that one unit of electric charge was exchanged. The observed weak interactions could be described in lowest order by the Lagrangian

$$\mathcal{L}_W = g \sum_a \bar{\psi}_a \gamma^\mu I^+ \psi_a W^-_\mu + g \sum_a \bar{\psi}_a \gamma^\mu I^- \psi_a W^+_\mu \qquad (1.14)$$

where the coupling constant g is related to the Fermi constant G_F through the mass m_W of $W^\pm$:

$$\frac{G_F}{\sqrt{2}} = \frac{g^2}{8m_W^2} \qquad (1.15)$$

and ψ_a are doublets of fermion fields, for example

$$\psi_e = \begin{pmatrix} \nu_e \\ e^- \end{pmatrix}, \ \psi_\mu = \begin{pmatrix} \nu_\mu \\ \mu^- \end{pmatrix}, \text{ etc.} \tag{1.16}$$

The operators $I^\pm$ are represented by the direct product of a Pauli matrix $\tau^\pm$ with the Dirac matrix $L = \frac{1}{2}(1 - \gamma_5)$ which projects out negative helicity:

$$I^\pm = \frac{1}{\sqrt{2}} (I_1 \pm iI_2), \ I_i = \frac{1}{2} \tau_i L, \ i = 1, 2, 3. \tag{1.17}$$

For a gauge invariant theory we must add a neutral gauge boson W^0 coupled to the neutral current constructed using the commutator I_3 of the operators $I^\pm$:

$$\mathcal{L}_{W^0} = g \sum_a \bar{\psi}_a \gamma^\mu I_3 \psi_a W^3_\mu. \tag{1.18}$$

The matrices I_i generate two dimensional unitary transformations on left handed fermions and the gauge group is called $SU(2)_L$. In a realistic theory we must also include electromagnetic couplings, but they cannot be added directly to (1.14) and (1.18) because the charge matrix Q already contains a piece proportionial to I_3. We enlarge the gauge group to include the full electromagnetic charge by defining a "hypercharge" operator

$$Y = Q - I_3 \tag{1.19}$$

which commutes with the I_i. We then add a coupling

$$\mathcal{L}_B = g' \sum_a \bar{\psi}_a \gamma^\mu Y \psi_a B^c_\mu \tag{1.20}$$

so that the gauge group becomes $SU(2)_L \times U(1)$, where the generator Y

of U(1), represented by

$$Y = QR + (Q - \frac{\tau_3}{2})L, \; R = \frac{1}{2}(1 + \gamma_5), \tag{1.21}$$

generates helicity dependent local phase transformations. The electromatnetic current is therefore split into two components Y and I_3 coupled, respectively, to B and W_3. Defining two orthornormal fields,

$$\begin{aligned} A_\mu &= B_\mu \cos\theta_w + W^3_\mu \sin\theta_w \\ Z_\mu &= W^3_\mu \cos\theta_w - B_\mu \sin\theta_w \end{aligned} \tag{1.22}$$

the sum of the interactions (1.18) and (1.20) can be rewritten as

$$\begin{aligned} \mathcal{L}_{W_0} + \mathcal{L}_B = {} & A_\mu \bar{\psi} \gamma^\mu [g' Q \cos\theta_w - I_3(g' \cos\theta_w - g \sin\theta_w)]\psi \\ & + Z_\mu \bar{\psi} \gamma^\mu [I_3(g \cos\theta_w + g' \sin\theta_w) - Q g' \sin\theta_w]\psi. \end{aligned} \tag{1.23}$$

Indentifying A_μ with the photon, which couples only to charge Q with strength e, gives

$$e = g' \cos\theta_w = g \sin\theta_w \tag{1.24}$$

and the Z-coupling reduces to the simple form

$$\mathcal{L}_Z = \frac{g}{\cos\theta_w} Z \bar{\psi} \gamma^\mu [I_3 - Q \sin^2\theta_w]\psi. \tag{1.25}$$

The neutral current interaction (1.30) was obtained by the minimal extension of the known couplings (1.1) and (1.14) to a gauge invariant theory. At the time when the now "standard" model was first proposed, neutral currents had not been observed, and alternative models were proposed which used the introduction of additional leptons and

quarks to eliminate Z-couplings to neutrinos (Lee 1972, Prentki & Zumino 1972) or to eliminate the Z entirely (Georgi & Glashow 1972). These models were less appealing on other grounds and were rendered obsolete by the discovery of neutral currents.

Returning to (1.25), the weak neutral couplings of fermions are seen to be completely specified by their charge and (helicity dependent) weak isospin in terms of a single parameter, the "weak angle" θ_w which characterizes the singlet-triplet mixing of the neutral vectors. At low energies transitions envolving massive boson exchange appear point-like with strength given by a Fermi constant G. Comparing (1.25) with (1.14), the relative strength of neutral and charged current effects is seen to be

$$G_Z/G_F = m_W^2 \cos^2\theta_w/m_Z^2. \tag{1.26}$$

At this point we must consider how vectors may acquire masses in a gauge invariant theory. One assumes that particle interactions are governed by a gauge invariant Lagrangian but that the lowest energy ("vacuum") state is not gauge invariant. Then the physical spectrum will not appear to satisfy the requirements of the gauge symmetry. According to a general theorem, (Goldstone 1961) this situation, known as "spontaneous symmetry breaking", implies the existence of massless scalars called "Goldstone bosons". In the case of a local gauge symmetry, the Goldstone scalars can be removed from the Lagrangian by a gauge transformation and their degrees of freedom reappear as the longitudinal components of those vectors which become massive. This phenomenon is known as the Higgs-Kibble mechanism (Higgs 1964, Kibble 1967).

The Higgs mechanism is most easily implemented by the introduction of scalar fields which transform under the gauge group. Let us add to the above model two coupled scalar fields (ϕ^+, ϕ^0) which transform as a doublet under $SU(2)_L$ with hypercharge $Y_\phi = \frac{1}{2}$. They couple to gauge vectors through the covariant derivative

$$|D_\mu \Phi|^2 = |(\partial_\mu - ig \frac{\vec{\tau}}{2} \vec{W}_\mu - i g' \frac{1}{2} B_\mu)\Phi|^2, \quad \Phi = \begin{pmatrix} \phi^+ \\ \phi^0 \end{pmatrix}. \tag{1.27}$$

In addition we add a "scalar potential" with $SU(2)_L \times U(1)$ invariant mass and interaction terms:

$$V = - \mathcal{L}_\phi = - \mu^2 \Phi^+ \Phi + \lambda (\Phi^+ \Phi)^2, \quad \lambda > 0. \tag{1.28}$$

If $\mu^2 < 0$, the bilinear term is an ordinary mass term and V has its minimum at $\Phi = 0$. For $\mu^2 > 0$, the minimum occurs for a value $\Phi \equiv \langle \Phi \rangle$ with

$$|\langle \Phi \rangle| = \frac{\mu^2}{2\lambda} \equiv \frac{v^2}{2} \tag{1.29}$$

In this case we must redefine the scalar field so that scalar excitations correspond to perturbations around the lowest energy state. Since Φ is characterized by four real functions we may write it as

$$\Phi = \exp\left(\frac{i\vec{\theta}}{v} \cdot \frac{\vec{\tau}}{\sqrt{2}}\right) \begin{pmatrix} 0 \\ \frac{H(x)+v}{\sqrt{2}} \end{pmatrix} \tag{1.30}$$

where θ_i and H are real and by definition $\langle H(x) \rangle = \langle \vec{\theta}(x) \rangle = 0$. This choice defines the direction of electromagnetic charge in the internal symmetry space: it is by definition the operator which leaves $\langle \Phi \rangle$ invariant. The potential (1.28) is independent of $\vec{\theta}$; excitation of these degrees of freedom corresponds to a rotation of Φ in isospin space and costs no energy. In the absence of gauge

interactions $\vec{\theta}$ would emerge as a massless Goldstone field with derivative couplings as determined by expanding the kinetic energy term $|\partial_\mu \Phi|^2$. Using instead the covariant derivative, gauge invariance ensures that

$$\mathcal{L}(\Phi,W,B,\psi) = \mathcal{L}(\Phi',W',B',\psi') \tag{1.31}$$

where the primed fields are obtained from the unprimed ones by a gauge transformation. Choosing as parameters $\lambda_i = -\theta_i$, $\lambda_0 = 0$ removes the fields θ_i from the Lagrangian as expressed in terms of ψ', B' and

$$W_i' = W_i + \frac{\sqrt{2}}{v}\partial_\mu \theta_i + \ldots \tag{1.32}$$

which now has a longitudinal component. The covariant derivative (1.27) now becomes (dropping primes on gauge fields)

$$|D_\mu \Phi'|^2 = \frac{1}{2}\left|D_\mu \begin{pmatrix} 0 \\ H+v \end{pmatrix}\right|^2 = \frac{1}{2}|\partial_\mu H|^2 + \frac{(H+v)^2}{2}\left(\frac{g^2}{2} W^+W^- + \frac{g^2}{4\cos^2\theta} Z^2\right). \tag{1.33}$$

The photon field A does not appear in (1.33) since it decouples from the neutral scalar; the squared coupling for the Z is taken from (1.25) with $I_3 = -\frac{1}{2}$, $Q = 0$. The last term in (1.33) determines the couplings of W and Z to the physical scalar field H and also their masses:

$$m_W^2 = \frac{g^2 v^2}{4} = \cos^2\theta_w m_Z^2. \tag{1.34}$$

Using this result in (1.26), we find equal effective Fermi constants for charged and neutral current couplings. This result follows from the $SU(2)_L$ doublet structure of Φ; a different transformation property

would have resulted in a different mass ratio and unequal coupling constants. Fermion masses may be generated by introducing Yukawa couplings of fermions to Φ; redefining the scalar field as in (1.30) gives rise to a fermion mass matrix proportional to v.

The electroweak gauge model with the specific symmetry mechanism described here is known as the standard model. It predicts the strength and structure of all neutral current phenomena in terms of a single parameter θ_w. Although it has met with remarkable experimental success, many theorists believe that the symmetry breaking mechanism may be more complicated. These possibilities are mentioned in section 6, but have little bearing on the physics of vectors which will be our main concern.

Before proceeding to the discussion of vector phenomenology, we must specify more completely the fermion content of the theory. At the time the electroweak theory was formulated, the data required three $SU(2)_L$ doublets of fermions: the two lepton doublets of (1.16) and one quark doublet (Gell-Mann & Levy 1960, Cabibbo 1963)

$$\psi_u = \begin{pmatrix} u \\ d_c \end{pmatrix} \tag{1.35}$$

where u is the "up" quark of charge $\frac{2}{3}e$ and d_c is a superposition of the "down" and "strange" quarks

$$d_c = d \cos\theta_c + s \sin\theta_c \tag{1.36}$$

of charge $-\frac{1}{3}e$. The "Cabibbo angle" θ_c is determined experimentally by comparing rates for semi-leptonic decays with strangeness change $|\Delta S| = 1$ and 0. The doublet (1.35) presented a difficulty for the

theory since its contribution to the neutral current (1.18) should be

$$\bar{\psi}_u \gamma^\mu I_3 \psi_u = \frac{1}{2}(\bar{u}\gamma^\mu Lu - \bar{d}_c \gamma^\mu L d_c) \tag{1.36}$$

which implied a strangeness changing neutral current coupling

$$\mathcal{L}_{\Delta S \neq 0} = \frac{g}{2} \sin\theta_c \cos\theta_c (\bar{d}\gamma^\mu Ls + \bar{s}\gamma^\mu Ld) W^3_\mu . \tag{1.38}$$

The coupling (1.37) would induce the decay $K_L \to \mu\mu$ at a rate comparable to that for $K^+ \to \mu + \nu_\mu$, while experimentally the $\mu^+\mu^-$ mode is suppressed relative to the $\mu\nu$ mode by a factor 4×10^{-9} in rate. Before the work of 't Hooft (1971), Glashow, Iliopoulos and Maiani (1970) had suggested that such strong suppression of strangeness changing neutral currents, which should occur at higher orders even in a theory with only charged weak currents, could be understood if there were a fourth "charmed" quark c of charge $\frac{2}{3}$ e which forms a weak isospin doublet with the superposition s_c of s and d orthogonal to d_c:

$$\psi_c = \begin{pmatrix} c \\ s_c \end{pmatrix}, \quad s_c = s \cos\theta_c - d \sin\theta_c \tag{1.39}$$

then the strangeness changing component of the neutral coupling

$$g\, \bar{\psi}_c \gamma^\mu I_3 \psi_c W^3_\mu \tag{1.40}$$

exactly cancels (1.38). Although there was no evidence for charmed hadrons, the development of renormalizable theories made a mechanism of the GIM type seem imperative. Studies of higher order contributions to neutral strangeness changing currents led to estimates (Vainshtein & Khriplovich 1973 , Gaillard & Lee 1974) of the masses of charmed hadrons and intensive experimental searches eventually established (Aubert et al 1974, Augustin et al 1974, Goldhaber et al

1976, Perruzzi et al 1977) their existence and confirmed their predicted properties. This discovery together with the discovery of neutral currents cemented the belief in gauge theories for many theorists. Indeed, it is generally believed that the strong nuclear interactions are also described by a gauge theory. In order to understand baryon spectroscopy and other low energy properties of hadron interactions, it has long seemed necessary to postulate that each of the "flavors" (u,d,s,c,...) of quark exist in three different varieties called colors. This new degree of freedom is believed to be gauged with massless vector bosons called gluons representing an $SU(3)_c$ color group. The resulting gauge theroy, called Quantum Chromodynamics (QCD) has had considerable qualitative success in describing how the strong interactions get weaker at high energies so that the quark constituents of hadrons appear essentially free. One particularly convincing manifestation of this property of asymptotic freedom was in the spectroscopy and decay properties of hadrons containing the relatively massive charm quark.

Along with the discovery of charm, the existance of an unexpected new lepton, the τ, was also revealed (Perl et al 1975). Data suggest that the τ couples weakly to a third neutrino forming a lepton doublet

$$\psi_\tau = \begin{pmatrix} \nu_\tau \\ \tau^- \end{pmatrix} \tag{1.41}$$

with the same couplings as ψ_e and ψ_ν. This discovery led to the postulate of yet another quark doublet

$$\psi_t = \begin{pmatrix} t \\ b \end{pmatrix}, \tag{1.42}$$

again on the grounds of renormalizability. In spite of gauge invariance, helicity dependent fermion-vector couplings induce infinities in higher order corrections to the three-vector vertex which can be removed only by cancellations among different fermions. The condition for this cancellation in the standard model is that the sum over fermion charges vanish. Since each quark doublet really represents three (mass and charge degenerate) doublets, corresponding to the three color degrees of freedom of the strong interaction gauge group $SU(3)_c$, the charge sum rule is satisfied if there are equal numbers of quark and lepton doublets which one tends to associate as "generations" of fundamental fermions. Hadrons apparently composed of b and $\bar{b}$ have been identified (Herb et al 1977), while evidence for the t quark is still being sought, and its non-observation to date means that its mass must be at least 18 GeV. The extension to six quarks had in fact already been proposed by Kobayashi and Maskawa (1973) because the Cabibbo mixing of b with d and s provides a possible source for the CP violating effects observed in K-decays.

To summarize, there is a large body of data (Hung & Sakurai 1981) which supports the belief that weak and electromagnetic interactions can be described together by a renormalizable gauge theory. However direct confirmation is still lacking. Aside from verifying the existence of the heavy vectors, many theorists believe the crucial test of the gauge theory postulate is the structure of their self couplings. In the standard model these arise uniquely from the Yang-Mills interaction

$$\mathcal{L}_{YM} = -\frac{1}{4} G^i_{\mu\nu} G_i^{\mu\nu}, \quad i = 1, 2, 3$$

$$G^i_{\mu\nu} = \partial_\mu W^i_\nu - \partial_\mu W^i_\mu + g\epsilon_{ijk} W^i_\mu W^k_\nu \tag{1.43}$$

which contains tri-linear and quartic couplings of the charged

$$W^{\pm} = \frac{1}{2} (W_1 \pm iW_2) \tag{1.44}$$

and neutral

$$W_3 = \cos\theta_w Z - \sin\theta_w A \tag{1.45}$$

intermediate bosons. Even accepting a gauge theory description, there are uncertainties which persist. For example, there is a class of models which mimic the minimal model at low energy but would show up as dramatically different in the spectrum of massive vectors.

This article will describe the physics of weakly coupled vectors. Section 2 covers their "static" properties: mass, decay widths and branching ratios. Subsequent sections treat production mechanisms: e^+e^- annihilation, lepton induced reactions on nucleons, pp and $p\bar{p}$ collisions. In Section 6 we briefly review the phenomenology of scalar particles associated with the clouded issue of symmetry breaking; the best laboratory for their study may in fact be in associated production with vectors or in their decay. Section 7 summarizes our conclusions.

II. GENERAL PROPERTIES OF THE VECTOR BOSONS

The previous section has described the arguments that led to the formulation of the "standard" model of weak and electromagnetic interactions, and has developed much of its structure. In this section we will start to focus on the physics of the as yet unseen vector bosons by listing some of their expected properties. Although experiments to date have been made in restricted kinematic ranges far from those where the vector bosons should appear, the manifold successes of the standard model and its tightly constrained nature tempt us to make the extrapolation and enable us to make relatively detailed predictions for their masses and decay modes.

2.1 Properties of the Charged Vector Bosons

We start with the charged vector bosons $W^{\pm}$, whose masses can be inferred from the known strength of the charged weak interactions:

$$\frac{G_F}{\sqrt{2}} = \frac{g^2}{8m_W^2} \tag{1.15}$$

and the magnitude of the SU(2) coupling constant g:

$$g = \frac{e}{\sin\theta_w} \tag{1.24}$$

in the standard model. Combining these two results we find

$$m_{W^{\pm}} = \sqrt{\frac{\pi\alpha}{\sqrt{2}G_F}} \quad \frac{1}{\sin\theta_w} \approx \frac{37.4\text{GeV}}{\sin_w} \tag{2.1}$$

The experimental value of the neutral weak mixing angle θ_w is such that $\sin^2\theta_w \approx 0.21$ to 0.25, corresponding to

$$m_W = 75 \text{ to } 82 \text{ GeV} \tag{2.2}$$

if we use the formula (2.1). This value is calculated directly from the Lagrangian without taking into account radiative corrections. Since the standard model is renormalizable, we are able to compute reliably to any desired order the radiative corrections to the formula (2.1) and the resulting prediction (2.2). The one-loop radiative corrections have recently been calculated (Bardin 1981, Veltman 1980, Sirlin & Marciano 1981, Llewellyn Smith & Wheater 1981). When used in the analysis of weak neutral current data they tend to reduce somewhat the preferred range of $\sin^2\theta_w$:

$$\sin^2\theta_w = 0.215 \pm 0.012 \begin{pmatrix}\text{radiative}\\ \text{corrections}\\ \text{included}\end{pmatrix} \tag{2.3}$$

and raise the prediction (2.2) for the $W^{\pm}$ boson mass by a few percent:

$$m_{W^{\pm}} = 83.0 \pm .24 \text{ GeV} \quad \begin{pmatrix}\text{radiative}\\ \text{corrections}\\ \text{included}\end{pmatrix} \tag{2.4}$$

The principal decay modes of the $W^{\pm}$ are also very easily deduced from the standard model Lagrangian of section 1. One finds for example that the leptonic decay mode $W^- \to e^- \bar{\nu}_e$ has the partial decay width

$$\Gamma(W \to e^- \bar{\nu}_e) = \frac{G_F m_{W^{\pm}}^3}{6\pi\sqrt{2}} \tag{2.5}$$

The partial rates for other fermion-antifermion decay modes are simply related to (2.5) if one neglects the effects of finite fermion masses. All such (m_f/m_W) effects are rather small when they involve the as yet unseen quark t, whose mass must be at least 18 GeV. One finds that

$$\Gamma(W^- \to e^- \bar{\nu}_e) : \Gamma(W^- \to \mu^- \bar{\nu}_\mu) : \Gamma(W^- \to \tau^- \bar{\nu}_\tau) : \Gamma(W^- \to \bar{q}q')$$
$$\approx 1 : \quad 1 : \quad 1 : 3|U_{qq'}|^2 \tag{2.6}$$

where the factor 3 in equation (2.6) is a counting factor arising because each quark pair $\bar{q}q'$ can be produced in three different colors. The quantity $U_{qq'}$ in equation (2.6) parametrizes the mixing (Kobayashi & Maskawa, 1973) of the charged weak current between the quarks q and q'. In the familiar cases of the up, down and strange quarks $U_{qq'}$ is essentially given by the well-known Cabibbo angle θ_c:

$$|U_{ud}| = \cos\theta_c, \quad |U_{us}| = \sin\theta_c \tag{2.7}$$

with a natural extension to a world with more quarks and mixing angles. The matrix of couplings $U_{qq'}$ is unitary in a space of dimensionality N_G equal to the total number of fermion generations. Since each doublet of colored quarks is accompanied in the standard model by a doublet of leptons, one expects on the basis of equation (2.6) that

$$\frac{\Gamma(W^- \to e^-\bar{\nu}_e)}{\Gamma(W^- \to \text{all})} = \frac{\Gamma(W^- \to \mu^-\bar{\nu}_\mu)}{\Gamma(W^- \to \text{all})} \approx \frac{1}{4N_G} \lesssim \frac{1}{12} \tag{2.8}$$

if all the fundamental fermions are much lighter than the $W^\pm$, and they have no other important decay modes. Indeed, fermion-antifermion pairs are by far the most important decay modes of the $W^\pm$ in the standard model, so that the results (2.8) stand as the predictions for the leptonic branching ratios. The total $W^\pm$ decay width can be estimated by substituting the expected mass (2.4) into the anticipated decay width for $W^- \to e^-\bar{\nu}_e$:

$$\Gamma(W \to e^-\bar{\nu}_e) \approx 260 \text{ MeV} \tag{2.9}$$

and then multiplying by $4N_G$, as suggested by equations (2.6) and (2.8).

One finds

$$\Gamma(W^- \to \text{all}) \approx N_G \text{ GeV} \tag{2.10}$$

which is significantly wider than the mass resolution which should be obtainable in some of the experimental searches discussed in subsequent sections. While comparatively large by hadronic standards, the width (2.10) is still only a few percent of the large mass (2.4) expected for the $W^{\pm}$, so that the $W^{\pm}$ can still be regarded as a "narrow" resonance.

2.2 Properties of the Z^0

Turning now to the Z^0, the expected mass can again be derived simply from the standard model as set out in Section I:

$$m_{Z^0} = \frac{m_{W^{\pm}}}{\cos\theta_w} = \sqrt{\frac{\pi\alpha}{\sqrt{2}G_F}} \frac{1}{\sin\theta_w \cos\theta_w} = \frac{37.4}{\sin\theta_w \cos\theta_w} \text{ GeV}. \tag{2.11}$$

As in the case (2.2, 2.4) of the $W^{\pm}$, this mass estimate is subject to significant radiative corrections. If one includes the radiative corrections to equation (2.11) one finds that

$$m_{Z^0} = 93.8 \pm 2.0 \text{ GeV} \tag{2.12}$$

Also as in the case of the $W^{\pm}$, one expects the principal decay modes to be fermion-antifermion pairs. We may parameterize the coupling of the Z^0 to a fermion pair $f\bar{f}$ ($f = e^-, \mu^-$, u, d, etc.) by:

$$\mathcal{L}_{Zf\bar{f}} = -\frac{m_Z}{\sqrt{2}} \left(\frac{G_F}{\sqrt{2}}\right)^{1/2} \bar{f}\gamma_\mu (v_f - a_f\gamma_5) f Z^\mu. \tag{2.13}$$

In the standard model (2.13) is equivalent to (1.25) with m_Z determined by (1.34) and (1.15), and the vector couplings v_f and axial couplings a_f are

$$a_\nu = v_\nu = 1 \text{ for neutrinos}$$
$$a_f = -1 \quad v_f = -1 - 4q_f \sin^2\theta_w \quad \text{for } q_f < 0 \tag{2.14}$$
$$a_f = 1 \quad v_f = 1 - 4q_f \sin^2\theta_w \text{ for } q_f > 0.$$

The various partial decay widths can be expressed in terms of the vector and axial couplings of equation (2.13):

$$\Gamma(Z^0 \to \bar{f}f) = \frac{G_F m_Z^3}{6\pi\sqrt{2}} (1 \text{ or } 3)\ (v_f^2 + a_f^2). \tag{2.15}$$

In view of the suppression of flavor-changing neutral currents, one expects the decay products to have equal and opposite flavors. The factor of 1 or 3 in (2.15) depends whether one is studying a leptonic decay mode or a quark-antiquark mode with its characteristic factor for the number of colors. Using the standard model neutral current couplings of Section I one finds (Camilleri et al 1976)

$$\Gamma(Z^0 \to \bar{\nu}_e \nu_e) : \Gamma(Z^0 \to e^+e^-) : \Gamma(Z^0 \to \bar{u}u) : \Gamma(Z^0 \to \bar{d}d)$$

$$= 2 : 1 + (1 - 4\sin^2\theta_w)^2 : 3\left(1 + \left(1 - \tfrac{8}{3}\sin^2\theta_w\right)^2\right) : 3\left(1 + \left(1 - \tfrac{4}{3}\sin^2\theta_w\right)^2\right) \tag{2.16}$$

and similarly for the second and third generation flavors if one neglects corrections of order m_f^2/m_W^2. These are not actually negligible (Marciano & Parsa 1981) for the top quark:

$$\Gamma(Z^0 \to \bar{t}t) = \frac{G_F m_{Z^0}^3}{4\sqrt{2}\pi}\left(1 - \frac{4m_t^2}{m_Z^2}\right)^{1/2}\left[1 - \frac{8}{3}x + \frac{32}{9}x^2 - \frac{m_t^2}{m_W^2}\left(1 + \frac{16}{3}x - \frac{64}{9}x^2\right)\right] \tag{2.17}$$

(where $x \equiv \sin^2\theta_w$) implies a reduction of 0(20)% by comparison with the decay rate into $\bar{u}u$ if the top quark has a mass of 20 GeV, close to the present experimental limit. If there were equal numbers of light fermions of the different charges (neutrinos, charged leptons, charge $+\frac{2}{3}$ quarks and charge $-\frac{1}{3}$ quarks, we would expect on the basis of equation (2.16) that

$$\frac{\Gamma(Z^0 \to e^+e^-)}{\Gamma(Z^0 \to \text{all})} = \frac{\Gamma(Z^0 \to \mu^+\mu^-)}{\Gamma(Z^0 \to \text{all})} \approx \frac{1}{11N_G} \lesssim 3\% \tag{2.18}$$

since we know there must be at least three generations. From the expected Z^0 mass (2.12) and the formula (2.15) for the partial decay widths, we deduce

$$\Gamma(Z^0 \to e^+e^-) \approx 90 \text{ MeV} \tag{2.19}$$

and

$$\Gamma(Z^0 \to \text{all}) \approx N_G \text{ GeV} \tag{2.20}$$

which is again considerably wider than the experimental resolution expected in some of the experimental searches. The total width (2.20) is slightly reduced by the finite mass correction (2.17) for the top quark, but this effect is compensated for by the QCD radiative corrections to the quark-antiquark decay modes, each of which is multiplied by a factor

$$\left[1 + \frac{\alpha_s}{\pi} + \ldots\right] \approx 1.04 \ . \tag{2.21}$$

The end result is to retain the simple formula (2.20).

A point of some phenomenological interest and uncertainty is the total decay rate into neutrinos:

$$\Gamma(Z^0 \to \sum_{\nu} \nu\bar{\nu}) = 0.18 \text{ GeV} \times N_{\nu}. \tag{2.22}$$

Neutrinos are of course much lighter than the related charged leptons, and we have very meager indications how many there may be: presumably they could all be produced in Z^0 decays even if their partner leptons were heavier than $\frac{1}{2}m_{Z^0}$. The most direct upper limit on the number of neutrinos from particle physics experiments probably comes from K^+ decays. The limit (Asano et al 1981)

$$\Gamma(K^+ \to \pi^+ \Sigma \nu\bar{\nu}) / \Gamma(K^+ \to \text{all}) \lesssim 1.4 \times 10^{-7} \tag{2.23}$$

corresponds (Ellis 1981) to an upper limit of

$$N_{\nu} \lesssim O(10^5) \tag{2.24}$$

A similar limit can be deduced from the success of simple QCD calculations of the total decay rate and e^+e^- branching ratio of the lightest known meson containing a b quark and its antiquark. By way of contrast, cosmological nucleosynthesis calculations (Steigman 1980) suggest that

$$N_{\nu} \lesssim 3 \text{ or } 4 \tag{2.25}$$

for neutrinos weighing less than an MeV or so. If the number of light neutrinos is not excessive, a comparison of equations (2.20) and (2.22) suggests that

$$\frac{\Delta\Gamma(Z^0 \to \text{all})}{\Gamma(Z^0 \to \text{all})} \approx 6\% \text{ per neutrino} \tag{2.26}$$

so that a precision measurment of the Z^0 width should be able to tell us how many neutrinos there are. Provincial particle physicists may trust this more than the nucleosynthesis limit (2.25). However, if the Z^0 is significantly wider than the expectation (2.20), we must be sure to have excluded the possible existence of other substantial decay modes of the Z^0. None have been found in the standard model: for example it has been calculated (Alles et al 1977, Albert et al 1980) that

$$\frac{\Gamma(Z^0 \to W^{\pm} + X)}{\Gamma(Z^0 \to \text{all})} \sim 2 \times 10^{-7} \qquad (2.27)$$

and even decays into the mythical Higgs boson are expected to have relatively small branching ratios:

$$\Gamma(Z^0 \to H^0 + \ell^+\ell^- \text{ or } \mu^+\mu^-) \lesssim 10^{-4} \quad \text{(Bjorken 1977)} \qquad (2.28)$$

$$\Gamma(Z^0 \to H^0 + \gamma) \lesssim 10^{-6} \quad \text{(Cahn et al 1979)} \qquad (2.29)$$

The prospects for counting the number of neutrinos therefore seem quite good in the context of the standard model.

What about deviations from the standard model? Alternative theories based on larger groups than the minimal SU(2) × U(1) of Section I generally have more neutral current interactions and hence more than one neutral vector boson. In quite a large class of theories the lightest of these is actually lighter than the single Z^0 of the standard model (Georgi & Weinberg 1978). Experiments at e^+e^- storage rings in particular are gradually increasing the lower bound on the mass of such a light Z^0, and decreasing the phase space available to

such models (Branson 1981). There is an alternative variation (Abbott & Farhi 1981) on the standard model which predicts that the Z^0 should have a significantly higher mass. In this scenario the SU(2) group of the weak interactions is supposed not to be spontaneously broken, and to be characterized by a strong coupling constant. The Z^0 and $W^{\pm}$ are then expected to be composite states with strong couplings analogous to the familiar ρ mesons of hadronic physics. The relation (1.15) between the masses and couplings of the $W^{\pm}$ and the observed Fermi constant G_F still holds as a first approximation, so we see that strongly-interacting $W^{\pm}$ and Z^0 must be heavier than the conventional expectations (2.4, 2.12) and then the formulae (2.5) and (2.15) tell us that the $W^{\pm}$ and Z^0 must also be considerably wider than the standard model expectations (2.10) and (2.20). This scenario is certainly very far-out, and has several unsolved technical problems (Abbott & Farhi 1981), but it serves to remind us that despite the strong circumstantial evidence for the standard model for the $W^{\pm}$ and Z^0, experiments may reveal to us something rather different.

III. VECTOR BOSON PRODUCTION IN ELECTION POSITION ANNIHILATION.

Most of the next generation of electron-positron colliders (see Table 1) are intended to be "Z^0 factories". The determination of the Z^0 mass will provide a precision measurement of the neutral weak mixing angle θ_w and/or a check of the higher order corrections discussed in Sec. 2, while the determination of its width counts otherwise undetectable weakly coupled light particles such as neutrinos. The hoped for production rate of about a million Z^0's per fortnight will allow searches for rare decay modes like those involving the elusive scalar bosons. All of these measurements can provide indirect probes of a still higher energy sector of the theory, just as precision measurements in kaon physics contributed important constraints on the construction of the electroweak theory of Section 1. In addition, the high rate of hadron production on resonance will provide a valuable laboratory for studies of both their weak and strong couplings. Here we emphasize straightforward tests of the electroweak theory at collision energies near the Z^0 pole, which will be described in Section III.1.

Production of charged intermediate bosons will not become significant until energies can be reached which are above the threshold for $e^+e^- \to W^+W^-$. The properties of this interaction, which directly probes the structure of the Yang-Mills couplings (1.43), will be described in Section III.2.

Most of the results presented in this section are taken from unpublished LEP studies (Camilleri et al 1976, and associated

LEP/ECFA reports). Additional unpublished material is contained in the Cornell Z^0 theory workshop (Peskin & Tye 1981).

III.1 Physics Around the Z^0 Pole.

In Section 2 we gave in equation (2.13) a general parameterization of the Z^0 couplings. The paramaters m_Z, v_f and a_f are in principle completely determined (up to an overall sign common to all the v's and a's) by measurements of the total cross section as a function of center of mass (c.m.) energy, the angular asymmetry of the final state momentum axis with respect to the beam axis, and polarization-dependent effects in the process

$$e^+e^- \to f\bar{f}. \tag{3.1}$$

Let us first consider the case where the final state pair is not e^+e^-. Then the process (3.1) will be dominated by single photon and Z^0 exchange in the direct channel. As is customary we shall normalize cross sections with respect to the lowest order one-photon exchange cross section:

$$\sigma_0 = \sigma(e^+e^- \to \gamma \to \mu^+\mu^-) = \frac{4\pi\alpha^2}{3s} = \frac{87}{s}\ \text{GeV}^2\ \text{nb} \tag{3.2}$$

where s is the total c.m. energy, and study the ratio

$$R_f = \sigma(e^+e^- \to f\bar{f})/\sigma_0 . \tag{3.3}$$

Then including both photon exchange and Z^0 exchange with the coupling (2.13) we obtain

$$R_f = q_f^2 - 2q_f v_e v_f \rho(s)\chi(s) + (v_e^2 + a_e^2)(v_f^2 + a_f^2)\rho^2(s)\chi(s) \tag{3.4}$$

where to simplify notation we have introduced the kinematic factors

$$\rho(s) = \frac{G_F}{8\sqrt{2}\pi\alpha}\ \frac{m_Z^2 s}{s-m_Z^2} \tag{3.5}$$

and

$$\chi(s) = \frac{(s - m_Z^2)^2}{(s - m_Z^2)^2 + \Gamma_Z^2 m_Z^2} \tag{3.6}$$

The factor $\chi(s)$ gives the Breit-Wigner smearing of the pole and can be set equal to unity in the narrow width approximation. The third term in (3.4) is the pure Z^0 contribution: the position and shape of the peak reflect the Z^0 mass and width, while the height of the peak determines the product of Ze^+e^- and $Zf\bar{f}$ coupling strengths. The second term arises from Z^0 and photon exchange interference and is sensitive only to the vector couplings of the Z^0 and its sign reflects the relative v_e/v_f sign. The relative contribution of vector and axial couplings can be read off from the value of R_f at the minimum which in the narrow width approximation occurs at

$$\rho(s) = \frac{q_f v_e v_f}{(v_e^2 + a_e^2)(v_f^2 + a_f^2)} \tag{3.7}$$

and takes the value

$$R_f^{min} = q_f\left(q_f - \frac{v_e v_f}{(v_e^2 + a_e^2)(v_f^2 + a_f^2)}\right) \tag{3.8}$$

The ratio R_μ ($q_f = -1$) is shown in fig. 1 for $m_Z = 83$ GeV and for several values of v and a where μ - e universality

$$v_e = v_\mu \equiv v, \quad a_e = a_\mu \equiv a \tag{3.9}$$

has been assumed. Note that universality alone predicts that the interference term has the same sign as $s - m_Z$. In the case of the standard model, Eq. (2.14), $v = 0$ for $\sin^2\theta_w = 0.25$, so that the presently favored value of $\sin^2\theta_w$ suggests that γ - Z interference

effects will be difficult to discern. For hadronic final states, their identification in terms of a primary $q - \bar{q}$ pair will be difficult at best, and realistic measurements of R_q will require an average over quark types of the interference effects which again are rather small if the parameters of the standard model are used.

More striking effects are expected in angular asymmetries which are more sensitive to axial couplings. Indeed, measurements at PETRA and PEP have already found indications of an axial coupling for the muon which is compatible with the standard model (Branson 1981). Defining θ as the angle between the incident e^- and the outgoing f, the differential cross section for (3.1) in the narrow width approximation is given by

$$\frac{d\sigma_f}{d\cos\theta} = \frac{\pi\alpha^2}{2s}\{q_f^2(1+\cos^2\theta) - 2q_f\rho(s)[v\,v_f(1+\cos^2\theta) + 2aa_f\cos\theta] + \rho^2(s)[(v^2+a^2)(v_f^2+a_f^2)(1+\cos^2\theta) + 8vav_fa_f\cos\theta]\}. \quad (3.10)$$

The integrated asymmetry, defined by

$$A_f = \frac{\int_0^1 d\cos\theta\,\frac{d\sigma_f}{d\cos\theta} - \int_{-1}^0 d\cos\theta\,\frac{d\sigma_f}{d\cos\theta}}{\int_{-1}^1 d\cos\theta\,\frac{d\sigma_f}{d\cos\theta}} \quad (3.11)$$

is given by the expression

$$A_f = \frac{3}{2}\,a\,a_f\rho(s)[-q_f + 2v\,v_f\rho(s)]/[q_f^2 - 2q_f\rho(s)vv_f + \rho^2(s)(v^2+a^2)(v_f^2+a_f^2)] \quad (3.12)$$

which vanishes if the axial coupling of either the electron or final

state fermion vanishes, and is bounded by $|A_f| < 0.75$. A_μ is shown in Fig. 2, assuming universality (3.9), for $m_Z^2 = 83$ GeV, $a^2 = 1$ and several values of v^2. At low energies $s \ll m_Z^2$, only the axial coupling is relevant and the effect is expected to be as large as 10% for energies $\sqrt{s} \simeq 40$ GeV charateristic of PEP and PETRA. Near the Z^0 pole, the shape of the asymmetry is sensitive to v^2/a^2. The asymmetry reaches its minimum value

$$A_\mu^{min} = -\frac{3}{4}\frac{a^2}{2v^2+a^2} \tag{3.13}$$

for $\rho = -\frac{1}{3v^2+a^2}$, and its maximum value

$$A_\mu^{max} = \frac{3}{4} \tag{3.14}$$

for $\rho = \frac{1}{a^2-v^2}$. As seen from Fig. 2, the effects are very pronounced and should yield precision measurements of a^2 and v^2. For hadronic final states, asymmetry measurements require some method of distinguishing jets of hadrons associated with a primary quark from those of an anti-quark. One method might be to measure the total charge of a jet. Then the quantity (3.11), with θ defined as the angle of a positively charged jet with respect to the incident e^- direction, would, to the extent that the jet charge "remembers" its parent quark charge, measure the weighted asymmetry

$$A_{Q_{jet}>0} = \frac{4}{5}\Sigma A_{q_f=\frac{2}{3}} - \frac{1}{5}\Sigma A_{q_f=-\frac{1}{3}}. \tag{3.15}$$

Another method is to assume that the fastest particle in a jet contains the primary quark; this again entails a weighted average over quark types. It seems plausible that at least consistency checks can be

made with regard to the axial and vector couplings predicted by the standard model. In the case where the final state fermion pair is e^+e^-, the process (3.1) recieves contributions from γ and Z^0 exchange in the crossed channel as well. The corresponding cross section and asymmetry formalae are considerably more complicated (see the above cited references) and we shall not reproduce them here.

With the assumption (3.9) of μ - e universality, the absolute magnitude and energy dependence of the cross section ratio R_μ and the asymmetry A_μ depend only on the three parameters $v,^2a^2$ and m_Z, and their measurement provides a check of universality. However no information on the sign of v/a can be obtained from these measurements; this requires some polarization-dependent information, which can be obtained either by measuring the final state lepton polarization (perhaps most realistically τ-polarization) or by comparing cross sections from left- and right-handed polarized incident beams.

In general, for unpolarized incident beams, the helicity of the final state fermion (averaged over production angle) is given by (again the narrow width approximation):

$$H^f(s) = -H^{\bar{f}}(s) = \frac{2\rho(s)a_f[q_f v_e - \rho(s)v_f(a_e^2 + v_e^2)]}{q_f^2 - 2q_f\rho(s)v_e v_f + \rho^2(s)(a_e^2 + v_e^2)(a_f^2 + v_f^2)} \tag{3.16}$$

On resonance this becomes

$$H^f(s) = -\frac{2a_f v_f}{(a_f^2 + v_f^2)} \tag{3.17}$$

providing a direct measurement of the sign as well as the magnitude of a/v for the final state fermion. A similar determination of a_e/v_e would be provided by measuring the dependence of the cross section rate on resonance as a function of the longitudinal polarization of the incident beam. Complete expressions for the angular dependence of the final state helicity and of the cross section for polarized beams have been given in the above cited references. Within the gauge theory context, the case for demanding polarized beams in the energy range around the Z^0 pole is in fact not very strong. The assumption of lepton universality allows the determination of the common parameter v/a from polarization measurements on a final state muon or τ. In this case the polarization is maximum in the forward direction, where for example, on resonance, the polarization attains the value

$$H^{\ell^-}(m_Z^2, \cos\theta = 1) = \frac{-4av(a^2+v^2)}{(a^2+v^2)^2+4av} \simeq 0.32, \qquad (3.18)$$

even for $v \simeq -0.12$ corresponding to $\sin^2\theta_w = 0.22$ in the standard model, so measurements of $H^{\ell}(s, \cos\theta)$ can provide a dramatic discriminator. While various suggestions which have been proposed (p-violating momentum correlations and polarization of leading particles of non-zero spin) for probing quark polarization do not appear very convincing as true quark polarimeters, such measurements are not actually necessary if the general form of the couplings (2.13) is accepted, since the possibly more feasible measurements of quark cross section ratios R_q and asymmetries A_q allow measurements of the signs as well as magnitudes of the quantities $a_q a_e$ and $v_q v_e$,

while universality (to be tested in A_ℓ- and R_ℓ-) together with the measurement of H^{ℓ^-} provides the sign of a_e/v_e.

More interesting phenomena may occur if the standard model is incorrect. Figure 3, taken from de Groot et al (1979), shows the shape of the cross section in a model where a second Z^0 is introduced whose couplings to fermions enter only through mixing effects with the standard Z^0 - leaving the low energy phenomenology of the standard model intact. In such a model similar exotic patterns would occur in the energy dependence of asymmetries and polarizations.

III.2 Production of Charged Intermediate Bosons.

The obvious way to measure the Yang-Mills couplings in e^+e^- collisions is through the process

$$e^+e^- \to W^+W^- \tag{3.19}$$

arising from direct channel Z^0 or photon exchange as in (3.1). As this requires a center of mass energy above the W^+W^- threshold, it is relevant to consider means of probing these couplings at lower energies. Their contribution to the cross section for the processes

$$e^+e^- \to e^\pm + W^\pm + \nu \tag{3.20}$$

has been calculated and found to be small for energies below the 2W threshold: For example

$$\sigma(e^+e^- \to We\gamma) \sim 10^{-7}\text{nb} \simeq 2 \times 10^{-5}\sigma_0 \tag{3.21}$$

in the standard model at $\sqrt{s} \simeq 150$ GeV, and the cross section falls rapidly at lower energies. The trilinear boson coupling contribution to

$$e^+e^- \to \gamma + \nu_e\bar{\nu}_e \tag{3.22}$$

has not been calculated, but is expected to be similar to (3.20) in order of magnitude. A possible probe of the ZWW vertex is through the decay

$$Z \to W + f\bar{f}' \tag{3.23}$$

where the fermion anti-ferion pair ($f\bar{f}' = e\bar{\nu}_e$, $\bar{u}d$, ...) arises from internal conversion of a virtual W produced at the ZWW vertex. The total branching ratio for processes of the type (3.23) is found to be only about 10^{-7}, giving a cross section (Alles et al 1977, Albert et al 1980)

$$\sigma(e^+e^- \to W + f\bar{f}') \sim 10^{-8}\text{nb} \sim 10^{-6}\sigma_0. \tag{3.24}$$

at $\sqrt{s} = m_Z$ where it is maximal.

We are therefore forced to consider the process (3.19) as the only feasible probe of the Yang-Mills couplings. The total cross section and angular distributions for this process have been calculated by Alles et al (1977) (see also Sushkov et al 1975) using the standard model, and detailed formulae are given in their paper. Figure 4 shows the cross section as a function of energy for several values of $\sin^2\theta_w$; with decreasing values of $\sin^2\theta_w$ the W^+W^- threshold increases (e.g. $\sqrt{s}_{th} = 170$ GeV for $\sin^2\theta = 0.20$) but the cross section peaks at a higher value. The angular distributions have also been given and show a strong asymmetry in $\cos\theta$(θ is defined as the W^- angle with respect to the e^- direction) which becomes increasingly pronounced with increasing c.m. energy. This effect is due to crossed channel ν_e

exchange, which is "uninteresting" compared to direct channel γ and Z exchange contributions because it involves only couplings that are already known from low energy data. Unfortunately ν_e exchange gives the dominant contribution for energies not far above threshold, as can be seen from Fig. 5 (Alles et al 1977), where different contributions to the cross section for (3.19) are plotted separately. However Fig. 5. also illustrates the sensitivity of the total cross section to the delicate cancellation required by a gauge theory: each of the interference terms gives a negative contribution comparable in magnitude to the square of each single exchange contribution.

In view of the importance of probing the Yang-Mills couplings, we must consider ways in which the different contributions may be separated. One useful tool in this respect is the use of longitudinally polarized beams. Since the ν-exchange contribution involves only left (right) handed electrons (positrons), the γ and Z^0 exchange contributions can be selected by colliding right-handed electrons with left handed positrons, for example, provided there is no contribution from right handed ν-exchange. In addition, the polarization of the final state W's, which can be analyzed using lepton angular distributions with respect to the W production axis, is also an effective probe. In particular, the coupling of longitudinally polarized W's would grow rapidly with c.m. energy in the absence of the cancellations assured by the Yang-Mills coupling of (1.43). These effects have been analysed in detail by Gaemers and Gounaris (1979) who give angular distributions for the different helicity amplitudes and show their

dependence on the trilinear coupling parameters. Should polarized beams not be feasible, one must rely on angular distributions to separate the different contributions. At fixed energy, the angular dependence of the lowest order Yang-Mills coupling is uniquely determined by the requirements of renormalizability, independently of the gauge group or symmetry breaking. If the only other contribution is the t-channel exchange of light ($m^2 \ll m_Z^2$, s) neutrinos there are only two independent amplitudes at fixed s, so that contributions to the cross section from s-channel gauge boson exchange, t-channel neutino exchange and their interference can be separated by weighted averaging of the data with suitably defined angular functions at each s. The s-dependence of the resulting functions will probe the structure of the gauge interactions. It turns out that the interference term, shown in Fig. 6 for three models, is the most sensitive probe. (An analysis of this type could be complicated by an additional contribution from cross channel exchange of doubly charge leptons and/or the exchange of appreciably massive fermions.) The error bars in Fig. 6 are based on 100 events per energy, which corresponds to about 250 running hrs. per energy for a beam lumiousity of 0.5×10^{32}/cm s in an experiment which triggers on one leptonic decay mode of the W. Since the dominant decay modes are expected to be hadronic, rates would be dramatically improved if hadronic decays of the W exhibit a clear enough two jet structure to permit detection above the annihilation background. Perrottet (1978) has discussed this possibility in detail and calculated jet angular distributions. Once the threshold for $e^+e^- \to Z^0Z^0$ is also passed, comparison of this reaction

(Brown et al 1979), which in the standard model proceeds only via cross channel lepton exchange, with reaction (3.19) should allow a further probe of the Yang Mills couplings contributing to the latter.

The higher order process

$$e^+e^- \to W^+W^-\gamma \tag{3.25}$$

receives contributions from quadrilinear vector boson couplings. Their detection might be feasible if c.m. energies well above 200 GeV can be attained. Contributions from electron bremsstrahlung can be suppressed by excluding small angle photons, and contributions involving ν-exchange with a tri-linear boson vertex could be eliminated if longitudinally polarized beams were available at the relevant energy. However the maximum value of the quadilinear coupling contribution to the cross section for (3.25) occurs at an energy

$$\sqrt{s} = 4m_W - m_Z^2 /4m_W = m_Z \left(4 - \frac{1}{4\cos^2\theta_W}\right) \simeq 300 \text{ GeV} \tag{3.26}$$

in the standard model if $\sin^2\theta_w \simeq 0.22$, and is only

$$\sigma_{max}(\text{quadrilinear}) \simeq 2 \times 10^{-7}\text{nb} \simeq 2 \times 10^{-4}\sigma_0. \tag{3.27}$$

While experiments of the type envisioned in this subsection will be difficult, it is clear that energies sufficiently high to allow multiple vector boson production can provide a unique and invaluable probe of the underlying electroweak theory.

Tabel 1 Comparison of e^+e^- colliding beam projects

Name	Location	Maximum center-of-mass energy (GeV)	Expected Luminosity ($cm^{-2}sec^{-1}$)	Status
LEP	CERN, Switz.	140(260)GeV	10^{32}	Approved
SLC	SLAC, USA	100 GeV	6×10^{30}	Proposed
CESR II	Cornell, USA	100 GeV	10^{32}	Proposed

IV. LEPTON-HADRON COLLISONS

We now turn to the manifestations of the weak vector bosons in very high energy lepton-hadron collisions. One can imagine experiments using any of three different types of leptons, either neutrinos, muons or electrons. High energy neutrino-hadron collisions could be studied using cosmic ray neutrino interactions in a very large underwater detector such as DUMAND (1982). Very high energy muon-hadron collisions could be studied using secondary muon beams obtained from a very high energy proton synchrotron such as the proposed VBA (Amaldi 1980). However, the best prospects for studying very high energy lepton-hadron interactions seem to be with electron-proton colliding beam machines, of which several are now being proposed (see Table 2). Weak vector bosons may manifest themselves in these reactions either indirectly through their propagator effects on cross-sections and on the interferences between neutral weak and electromagnetic interactions, or directly through production of the weak vector bosons in the final state. Since the cross-sections for the production of the $W^{\pm}$ and Z^0 are not very high, much of the interest in their signatures in lepton-hadron collisions centers on their indirect propagator effects, to which we now turn.

Low energy weak interaction amplitudes are proportional to the Fermi constant G_F, whose relation to the masses and couplings of the weak vector bosons we have already seen:

$$\frac{G_F}{\sqrt{2}} = \frac{g^2}{8m_W^2} = \frac{g^2 + g'^2}{8m_Z^2} \qquad (4.1)$$

At high energies the four-momentum q_μ transferred between the incoming and outgoing leptons may no longer be negligible compared with the vector boson mass. In this case the weak interaction amplitudes are proportional to

$$\frac{1}{m^2_{W^\pm} + Q^2} \quad \text{or} \quad \frac{1}{m^2_{Z^0} + Q^2} \tag{4.2}$$

where $Q^2 \equiv - q^2$ is the modulus of the space-like four-momentum transfer squared. This means that charged current weak interaction cross-sections will no longer rise like the square of the center-of-mass energy $s \equiv (p_\ell + p_h)^2$, as they do at low energies:

$$\sigma(\ell + h \to \ell' + X) \propto G_F^2 s \tag{4.3}$$

when $s \ll m^2_{W^\pm}$ if one assumes that strong interaction effects are negligible at large momentum transfers. One does not in fact expect these effects to be entirely absent, and the standard asymptotically free gauge theory of the strong interactions, namely QCD, leads one to expect logarithmic corrections to (4.3) at high momentum transfers Q^2. These are to be contrasted with the power-law Q^2 dependences to be expected (4.2) from the vector boson propagators. Furthermore, the propagator effects (4.2) are independent of parameters of the hadronic kinematics, whereas the QCD scaling violations are not universal functions of Q^2. For these reasons, it is in principle possible to disentangle vector boson propagator effects from conventional QCD effects.

Attempts have been made using present-day accelerator data either to establish a lower limit on the mass of the $W^{\pm}$, or even to determine that it is finite. These experiments are very difficult since the values of Q^2 ($\lesssim$ 400 GeV^2) presently available are much lower than the expected $W^{\pm}$ boson mass squared, and so far they have not yielded any positive results. The best published limit (Barish 1978) on the W boson mass is

$$m_{W^{\pm}} > 36 \text{ GeV}, \tag{4.4}$$

while a preliminary analysis of (Wahl 1981) CERN-Dortmand-Heidelberg-Saclay (CDHS) collaboration data suggests

$$m_{W^{\pm}} > 100 \text{ GeV} \pm \text{systematic effects}. \tag{4.5}$$

This result should not yet be construed as conflicting with the expected mass of order 80 GeV, since so far the analysis only takes into account statistical errors in the data, but does not yet take into account systematic errors. One can expect that the lower bound (4.5) will be decreased when these are included. It is possible that $W^{\pm}$ propagator effects may be detected in neutrino-hadron scattering data to be obtained at the FNAL tevatron in a few years time. However, the main hope for detecting these effects rests with ultra-high energy cosmic-ray neutrinos and electron-proton colliding ring machines.

Figure 7, taken from an analysis made for the DUMAND (1982) project, indicates how one may be able to detect $W^{\pm}$ propagator effects in ultra-high energy (0(10)TeV) cosmic ray neutrino interactions.

The up coming muons originate from neutrinos which have passed through the Earth. Their number is diminished by absorption, which is less significant if the neutrino cross-section rises more slowly than linearly (4.3) at high energies, as would be the case if $m_W \approx 80$ GeV. Stronger absorption effects occur if there are no W propagator effects (4.2), as would be the case if $m_W \gg 80$ GeV. In principle, measurements of the reaction $e^{\pm} + p \rightarrow \overset{(-)}{\nu} + X$ with a high-energy colliding beam machine can provide better determined kinematical conditions in a comparable range of center-of-mass energies. As an example, colliding 30 GeV electrons with 820 GeV protons as proposed with HERA (ECFA & DESY 1979) provides a center-of-mass energy $\sqrt{s} = 314$ GeV which corresponds to a lepton beam of 52 TeV striking a fixed target. Figure 8 shows the number of events expected per day at HERA of the reaction $e_L^- + p \rightarrow \nu_e + X$, binned in different ranges of Q^2. The event rates for a conventional $W^{\pm}$ mass of about 80 GeV and for an infinite $W^{\pm}$ mass are clearly very different, and it is believed that one could measure indirectly the $W^{\pm}$ mass to an accuracy of a few percent. It is also possible to look beyond the conventional $W^{\pm}$ to see if there are any more charged weak bosons $W^{\pm\prime}$. For example, if the simple $W^{\pm}$ propagator (4.2) were replaced by

$$\frac{1}{m^2_{W^{\pm}} + Q^2} \rightarrow \frac{1}{2}\left[\frac{1}{m^2_{W^{\pm}} + Q^2} + \left(\frac{m^2_{W^{\pm}\prime}}{m^2_{W^{\pm}}}\right)\left(\frac{1}{m^2_{W^{\pm}\prime} + Q^2}\right)\right] \qquad (4.6)$$

so that one half of the low Q^2 amplitude were due to $W^{\pm\prime}$ exchange, then experiments with a machine such as HERA could (ECFA & DESY 1979) tell the difference between $m_{W^{\pm}\prime} = 500$ GeV and infinity.

One can also look for Z^0 propagator effects in high energy neutral current reactions. Here measurements are simplest in high energy electron and muon-hadron scattering, where one can easily know the kinematics of both the incoming and outgoing leptons. The picture is however complicated by the dominance of photon exchanges at low Q^2 and by important interference effects:

$$\sigma(\gamma + Z^0) \propto |A|^2 = \left| \frac{\hat{A}_{em}}{Q^2} + \frac{\hat{A}_{weak}}{m_{Z^0}^2 + Q^2} \right|^2 . \qquad (4.7)$$

At low $Q^2 \ll m_Z^2$ the interference effects are of order $10^{-5} Q^2 (GeV^2)$ and hence very small. They have been measured in two experiments: the classic SLAC experiment (Prescott et al 1978) demonstrating parity violation in deep inelastic ep scattering at $Q^2 = O(1) GeV^2$, and more recently a CERN experiment (Bollini et al 1982) which gives indications of a charge asymmetry in deep inelastic $\mu^{\pm} N$ scattering at $Q^2 = O(10^2) GeV$. Both these experiments are at Q^2 much too small to offer a hope of seeing Z^0 propagator effects which would cause a deviation from linearity with Q^2 in the interference effects. At high energy electron-proton colliding beam machines the electromagnetic and weak contributions (4.7) to the deep inelastic scattering cross-sections are comparable; dramatic interference effects should be seen and the Z^0 propagator clearly identifiable. Figure 9 shows (Ellis et al 1978) the ratios between the cross sections for different electron polarization states, both with and without the finite-mass Z^0 propagator (4.2). As in the case of the $W^{\pm}$, measurements with high energy ep colliding beams should be able to determine

indirectly the mass of the Z^0 to within a few per cent, and look for the indirect effects of further $Z^{0'}$s with masses of a few hundred GeV.

Looking for indirect effects of the $W^{\pm}$ and Z^0 through their propagators (4.2) is all very well, but it would be much more satisfying to see them produced directly. Unfortunately the cross-sections expected in high energy ep collisions are discouragingly small, although the cleanliness of many of the final states relative to those encountered in hadronic collisions alleviate some of the detection problems. The most important Feynman diagrams for the production of $W^{\pm}$ and Z^0 are shown in Figure 10. The diagrams of classes (a) and (b) where the $W^{\pm}$ or Z^0 are emitted from the leptonic vertex are expected to be accompanied by a relatively simple hadronic system which will often be just a proton or a nucleon resonance. This enables one to plan searches for all decay modes of the $W^{\pm}$ and Z^0, and not just their relatively disfavored (2.8, 2.18) leptonic decay modes. On the other hand the "hadronic" diagrams of class (c) can be expected to yield quite a complicated hadronic system, among which only leptonic decays of the $W^{\pm}$ and Z^0 may be discernible.

The cross-sections for leptoproduction of $W^{\pm}$ and Z^0 do not have simple analytic forms, and complete calculations of their production with ep colliding beams have not in fact been performed. The production cross-sections have been estimated (Llewellyn Smith & Wiik 1977) by scaling up old calculations for producing light $W^{\pm}$ and Z^0 at lower energy accelerators, or alternatively (Kamal et al 1981) using the Weizsäcker-Williams approximation to treat the photon

exchanged in figure 10. This latter method gives somewhat larger cross-sections than the previous one, but it is not clear whether the Weizsäcker-Williams approximation is appropriate for this calculation, so we prefer to be conservative and quote the old rescaled calculations. The cross-sections for the relatively clean events corresponding to emission from the leptonic vertices of Figs. 10 a, b are plotted in figure 11 as a function of $s/m^2_{W^\pm}$ and $s/m^2_{Z^0}$. Taking the values of $s/m^2_{W^\pm} = 15$ and $s/m^2_{Z^0} = 12$ appropriate to HERA we estimate (Llewellyn Smith & Wiik 1977, Ellis et al 1978)

$$\begin{aligned} \sigma(e^- + p \to \nu + W^- + p)_{\text{leptonic}} &\approx 2 \times 10^{-38}\,\text{cm}^2 \\ \sigma(e^- + p \to \nu + W^- + X \neq p)_{\text{leptonic}} &\approx 4 \times 10^{-38}\,\text{cm}^2 \end{aligned} \tag{4.8}$$

while

$$\begin{aligned} \sigma(e^- + p \to e^- + Z^0 + p)_{\text{leptonic}} &\approx 3 \times 10^{-37}\,\text{cm}^2 \\ \sigma(e^- + p \to e^- + Z^0 + X \neq p)_{\text{leptonic}} &\approx 2 \times 10^{-37}\,\text{cm}^2 \end{aligned} \tag{4.9}$$

It would probably be possible to detect the Z^0 with the cross-sections (4.9), but detecting the $W^\pm$ with the cross-sections (4.8) seems a rather more doubtful proposition. However, perhaps it is worth noting that the $W^\pm$ cross-sections are sensitive to the magnetic moment κ of the $W^\pm$. Changing the canonical gauge theory value of $\kappa = -1$, derived from (1.43), to $\kappa = 0$ decreases the expected cross-section by 10%, while changing to +1 increases the cross-section by 30%. In principle, observations of the reaction $e^+e^- \to W^+W^-$ have a greater sensitivity to the magnetic moment of the $W^\pm$, but it is only with a second higher energy phase of LEP that this reaction will become accessible.

We close this section by returning to Table 2 which lists different high energy electron-proton colliding beam projects that are known to us, together with some of their cruial parameters. The highest center-of-mass energy and luminosity are expected for HERA, which is not surprising since it is a device dedicated to ep physics, unlike all the other projects except TRISTAN which are secondary adjuncts to accelerators primarily intended for e^+e^- or hadron-hadron collisions. On the other hand, these parasitic projects are all much cheaper than HERA. At present neither HERA nor any of the other projects has been approved, and their prospects are somewhat uncertain.

Table 2 Comparison of ep Colliding Beam Projects

Name	Location	Maximum center-of-mass energy (GeV)	Expected Luminosity($cm^{-2}sec^{-1}$)
TRISTAN	KEK, Japan	173	1.8×10^{31}
HERA	DESY, Germany	314	6×10^{31}
Proposal 659	FNAL, USA	200	4×10^{31}
CHEER	FNAL, USA	200	$(1.7 \text{ to } 2.7) \times 10^{31}$
SPS/LEP	CERN, Switz.	249	1.3×10^{31}
ISABELLE	Brookhaven, USA	126	2×10^{31}

V. HADRON-HADRON COLLISIONS

Hadronic collisions are not as clean as e^+e^- or even ep collisions for making a thorough study of the predicted weak bosons, however they will provide higher energies at which these heavy objects should be produced more easily. Unlike e^+e^- collisions, the initial state interaction is not simple, since hadrons are made of quarks and gluons which interact strongly, presumably according to today's orthodoxy of QCD. Therefore all the calculations of weak boson production will call upon a model of the hadrons in terms of its constituents, which play the role of the incoming e^+e^- to create the weak bosons. Once these are produced, they will decay in the usual way as dictated by the electroweak theory. Unfortunately, these decays are just a very tiny part of the possible final states in hadronic collisions. In the haystack of all produced states we have to look for the characteristic "needle" signatures which are evidence for weak boson production. In recent years a large amount of literature has been devoted to this subject in connection with the various high energy pp and $p\bar{p}$ collider projects listed in Table 3. At BNL, ISABELLE, a proton-proton collider with center of mass energy $\sqrt{s}$ = 400-800 GeV, is under construction, while at FERMILAB a proton-antiproton machine with $\sqrt{s}$ = 2000 GeV is planned, using the Tevatron. In Europe, the SPS $p\bar{p}$ collider ($\sqrt{s}$ = 540 GeV) is now under operation and the first collisions have been observed, which may make the discovery of the weak bosons, if they exist, very imminent. In this section we give an overview of the physics of the weak bosons in pp and $p\bar{p}$ collisions without going

into more technical details which can be found in the literature by the interested reader.

5.1 Total Cross Sections for the Production of Weak Bosons.

The starting point for weak boson production is the Drell-Yan model (Drell & Yan 1971) which was originally intended to describe lepton-pair production in hadronic collisions. A quark from one colliding hadron and an antiquark from the other fuse into a virtual photon which in turn decays into a lepton pair (see Figure 12). In the naive version of the model (Feynmann, 1972) quarks and antiquarks are supposed to be essentially free objects inside the hadrons. However one knows that strong interaction corrections estimates using QCD are to be included in the calculations. Nevertheless, we shall use the naive model to present ballpark estimates and comment on the influence of QCD corrections on this Born approximation when necessary. In our case of interest we can follow the same physical picture as in lepton-pair production via a virtual photon; the only change is that we consider different elementary fusion subprocesses. At the constituent level the relevant subreactions are the following (Peierls et al 1977, Quigg 1977):

$$u\bar{u}, d\bar{d}, s\bar{s} \ldots \rightarrow Z_0;\ u\bar{d}, u\bar{s} \ldots \rightarrow W^+;\ \bar{u}d, \bar{u}s \ldots \rightarrow W^- \qquad (5.1)$$

if we neglect the small contributions of heavier quarks in the proton and the antiproton, which are expected to be relatively rare. The hadronic cross-section is obtained as an incoherent sum of all possible fermion subprocesses weighted by the respective probability distributions of the incoming constituents (see Fig. 13 for the

kinematics):

$$\frac{d\sigma}{ds}(A+B \to W+X) = \sum_{a,b} \int_0^1 dx_a \int_0^1 dx_b \, \delta(x_a x_b s - \hat{s}) f_{a/A}(x_a) f_{b/B}(x_b) \hat{\sigma}(a+b \to W) \tag{5.2}$$

where careted variables refer to the subprocess and $f_{a/A}(x_a)$ is the probablility of finding the consituent a inside the hadron A carrying a fraction x_a of the parent hadron's longitudinal momentum. From (5.2) we can study any kind of distribution for a definite final state provided we replace $\hat{\sigma}(a + b \to W^-)$ by the relevant subprocess distribution. For instance, the total cross-section for producing a W^+ is easily calculated, knowing that

$$\hat{\sigma}(a + b \to W^+) = \sqrt{2}\, G_F \pi \tau s \delta(\hat{s} - M_W^2) \tag{5.3}$$

which when substituted into equation (5.2) yields

$$\sigma(A + B \to W^+ + X) = \sqrt{2}\pi\, G_F \tau \int_\tau^1 \frac{dx}{x} \mathcal{L}^+(x, \tau/x) \tag{5.4}$$

where

$$\mathcal{L}^+(x,\tau/x) = \frac{1}{3}\{[u_A(x)\bar{d}_B(\tau/x) + \bar{d}_A(x)u_B(\tau/x)]\cos^2\theta_c$$

$$+ [u_A(x)\bar{s}_B(\tau/x) + \bar{s}_A(x)u_A(\tau/x)]\sin^2\theta_c\} \tag{5.5}$$

In equation (5.5) we have denoted the distribution function of a given quark by its own symbol. We remark that the total cross-section only depends on the dimensionless variable $\tau = \frac{M_W^2}{s}$. For the W^- case we interchange quark and antiquark densities, whereas for Z^0 production, the corresponding function $\mathcal{L}^0(x, \tau/x)$ is slightly more complicated because of the weak-electromagnetic mixing

$$\mathcal{L}(x,\tau/x) = \frac{1}{3}\{[u_A(x)\bar{u}_B(\tau/x) + \bar{u}_A(x)u_B(\tau/x)][\frac{1}{4} - \frac{2}{3}\sin^2\theta_w + \frac{8}{9}\sin^4\theta_w] +$$

$$[d_A(x)\bar{d}_B(\tau/x) + \bar{d}_A(x)d_B(\tau/x) + s_A(x)\bar{s}_B(\tau/x) + \bar{s}_A(x)s_B(\tau/x)]$$

$$\times [\frac{1}{4} - \frac{\sin^2\theta_w}{3} + \frac{2}{9}\sin^4\theta_w]\} \qquad (5.6)$$

The factors of $\frac{1}{3}$ in equations (5.5) and (5.6) account for the color degree of freedom. Charge invariance tells as that quark (antiquark) densities in a proton are the same as antiquark (quark) densities in an antiproton. In this simple picture $p\bar{p}$ collisions generally offer more constituent luminosity than pp collisions because the three "valence" quarks (anti-quarks) which carry the $p(\bar{p})$ quantum numbers also carry most of its its momentum, but this enhancement does not apply at very low values of τ where the "sea" of q-$\bar{q}$ pairs (and gluons) is important. For the planned colliders the larger luminosity available in proton-proton collisions may overcome this drawback and provide a larger absolute event rate than the proton-antiproton colliders.

A convenient variable for parametrizing the final state distribution is the rapidity which measures the longitudinal momentum of the produced weak boson

$$x_a - x_b = 2\sqrt{\tau}\ \text{sinhy}, \text{ i.e. } y = \frac{1}{2}\,\ell n\,\frac{E_\omega + p_{11}}{E_\omega - p_{11}} \qquad (5.7)$$

Distributions in this variable reflect the longitudinal distribution of the constituents, and for instance in pp collisions one expects a maximum away from y = 0, since the valence quarks carry more momentum than the sea anti-quarks and the W moves in the direction of the valence quarks. So far we have neglected strong interaction effects,

but in fact quarks can radiate gluons and hadrons contain gluons, and therefore there are additional diagrams to be considered (Reya 1981) as in Figure 14. The main effect of gluon radiation is to soften the quark distribution; that is, the low x region is more populated and the large x region is depressed. This evolution of the distribution is energy-momentum dependent, so that constituent distributions have a logarithmic dependence on the energy scale associated with the process as shown in Figure 15.

$$f_{a/A}(x) \rightarrow f_{a/A}(x, Q^2)$$

To leading order in $\frac{1}{\ell n Q^2}$ the momentum scale Q^2 is specified only up to a scale factor of order 1, but it seems physically reasonable to take $Q^2 = \hat{s}$, the energy of the constitutent reaction. Another effect of gluon emission is to give the W a transverse kick much larger than that expected from the Fermi motion of the constitutents inside the hadrons. These strong interaction refinements have been included in the caluclation of the total cross sections shown in Figure 16 (Paige 1979).

Logarithmic corrections are not important for $\sqrt{s} \sim 500 - 1000$ GeV since there the average fraction of energy carried by the constituents is $\langle x \rangle \sim \sqrt{\tau} \sim 0.1$ or 0.2, a region in which the constituent distribution functions are not greatly affected. However, for larger values of $\sqrt{s}$, as at the FNAL Tevatron, one expects a substantial increase of the cross-sections.

As a final remark let us point out that it has been realized that virtual gluon exchange induces a multiplicative correction factor to

the Drell Yan cross section which is of order O(2)(Altarelli et al 1979). An enhancement of this magnitude has in fact been seen in hadronic lepton-pair production. We have not taken this factor into account in the estimation; its effect would be to increase substantially the present estimates but not to modify the shape of the calculated distributions (Humpert & van Neerven 1980).

5.2 Leptonic Final States

Among all possible decays of the weak bosons, their leptonic modes are the easiest to select for a final state analysis. As indicated in section 2 the branching ratios into charged leptons in a three generation model are

$$B(Z^0 \to e^+e^- \text{ or } \mu^+\mu^-) \sim 3\% \quad B(W^+ \to \ell^{\pm}(\overset{-}{\nu}_{\ell}) \sim 8\% \qquad (5.8)$$

For an intergrated luminosity of 10^{36}cm $^{-2}$ this gives for $Z^0 \to \ell^+\ell^-$ ($W^{\pm} \to \ell^{\pm}$) at the $p\bar{p}$ collider ($\sqrt{s}$ = 540 GeV) about 23 events (60 events): a seeable signal even in this rather disfavored case. For lepton-pair production by the Z^0 the competing mechanisms are the usual Drell-Yan one via a virtual photon and the leptonic decays of heavy quarks like c and b(t?). Fortunately these backgrounds are much below the nice expected peak in the lepton-pair mass spectrum at the Z^0 mass (Figure 17)(Pakvasa et al 1979). The situation is less favorable for the leptonic modes of the charged weak bosons $W^{\pm}$ because of the emitted (anti)neutrino which escapes detection. However, if we consider the single charged spectrum, kinematics conspires in our favor. Denoting the momentum of the charged lepton

by ℓ, we look at the following distribution

$$\ell^0 \frac{d^3\sigma}{d\vec{\ell}} = \sum_{a,b} \int dx_a dx_b \; f_{a/A}(x_a) f_{b/B}(x_b) \ell^0 \frac{d^3\hat{\sigma}}{d\vec{\ell}} \; (a + b \to W^{\pm} \to \ell^{\pm} x)$$

$$= \sum_{a,b} \int \frac{d\hat{s}}{\hat{s}} \; \frac{f_{a/A}(x_a) f_{b/B}(x_b)}{\sqrt{1 - 4\ell_T^2/\hat{s}}} \; \frac{\ell_T^2}{\hat{s}} \; |M|^2 \qquad (5.9)$$

(where $|M|^2$ is the squared matrix element of the subprocess which contains the W propagator, ℓ_T is the momentum component perpendicular to the incident beam) and expect that the largest contribution will come from the region $\hat{s} \simeq M_W^2$. The denominator in equation (5.9) should lead to a sharp peaking of the cross-section at $\ell_T \sim \frac{M_W}{2}$, which is known as the Jacobian peak and is a very distinctive feature of a heavy object decaying into two light fermions (Figure 18). In the limit of zero width for the $W^{\pm}$ the ℓ_T spectrum would be cut off at $\frac{M_W}{2}$, but there are some smearing effects. First the finite width of the $W^{\pm}$, and secondly the intrinsic transverse momentum of the constituents and the QCD corrections which can give a rather significant transverse kick to the weak boson (Pakvasa et al 1979, Aurenche & Lindfors 1981). This latter contribution enlarges the available phase space for the lepton and we expect a smearing of the peak with events at $\ell_T > \frac{M_W}{2}$. Fortunately, the Jacobian peak should still emerge from the above-mentioned backgrounds, but it will be difficult to infer the W mass from the position of the maximum.

Once one has observed peaks in some distributions one would like to pin-point the specific characteristics of the weak bosons which

include the vector and axial pieces of their couplings introduced in section 1. In $p\bar{p}$ collisions a clear signal of the axial-vector interference is the forward-backward asymmetry of the lepton spectrum, the forward hemisphere being defined by the proton beam direction. More precisely, the asymmetry can be defined as:

$$A_{F-B}(s, \cos\theta) = \frac{\frac{d\sigma}{d\cos\theta}(\cos\theta) - \frac{d\sigma}{d\cos\theta}(-\cos\theta)}{\frac{d\sigma}{d\cos\theta}(\cos\theta) + \frac{d\sigma}{d\cos\theta}(-\cos\theta)} \qquad (5.10)$$

In the W case one expects this asymmetry to be large because of the pure (V-A) coupling and the qualitative effect can be visualized easily on the basis of helicity arguments. For instance we know that W^+ is mainly produced by the collisions u_L (from the proton)$\bar{d}_L$ (from the antiproton) which fixes the helicity of W^+. Since the outgoing neutrino is left-handed one clearly sees that the ℓ^+ will tend to be emitted along the direction of the antiproton beam (into backward hemisphere)(Figure 19). The asymmetry of ℓ^+ is therefore negative, whereas for the ℓ^- coming from W^- the situation is just the reverse. Sea quarks and QCD contributions can slightly modify the results for this observable but its qualitative features are still preserved. In Figure 20 we present the forward-backward asymmetry (Perrottet 1978, Finjord et al 1981) for the W^- case as a function of $\cos\theta$ for various values of $\tau = s/M_W^2$.

For the Z^0 this asymmetry will be more difficult to measure because the vector coupling to the lepton is proportional to $(1/4-\sin^2\theta_w)$ and is rather suppressed for today's value of

$\sin^2\theta_w \sim 0.215$. The predicted value of A_{FB} is about 7% and detecting such a low value calls for rather large statistics which will be difficult to achieve in the near future.

5.3. Hadronic Final States

As described in section 2, the weak bosons will decay most of the time into hadronic modes, and we therefore expect pairs of hadronic jets at large transverse momentum with a weak origin, to be distinguished from the formidable QCD background arising for quark and gluon scattering reactions characterized by the strong coupling constant $\alpha_s(M_w^2) \sim 0.1$ to 0.2, to be compared with weak one $\alpha_w = \sim 3 \times 10^{-2}$. We expect that the strong interaction two-jet cross section will dominate the weak one (Figure 21) by a large factor. The situation looks desperate unless we can devise a clever criterion to disentangle the two types of cross-sections. An interesting possibility is to look for heavy quark jets, since the weak bosons are heavy enough to decay in essentially the same way into light or heavy quarks (provided the unseen top quark is not too heavy). This would reduce the QCD background to the extent that we are able to distinguish a heavy quark jet from a light quark jet. In particular for the W^- decaying into $b\bar{t}$ the only competing QCD mechanism comes from $t\bar{t}$ and $b\bar{b}$ pairs. If we further require the observation of two energetic leptons of the same sign, the W^- signal can emerge from the background (Abud et al 1978, 1979). The decay chains are the following

$$W^- \to b\bar{t} \begin{cases} \nearrow \bar{b}\ell^-\bar{\nu}_\ell \\ \searrow c\ell^-\bar{\nu}_\ell \end{cases} \tag{5.11}$$

$$\text{QCD} \begin{cases} \nearrow t\bar{t} \begin{cases} \nearrow b\ell^-\bar{\nu}_\ell \\ \searrow b\to c\ell^-\bar{\nu}_\ell \end{cases} \\ \searrow b\bar{b}\to c\bar{c}\to s\ell^-\bar{\nu}_\ell \\ \qquad\searrow c\ell^-\bar{\nu}_\ell \end{cases} \tag{5.12}$$

The QCD mechanism involves cascade decays and therefore less energetic like sign leptons than those from the direct decays in the W^- case. Also the W^+ is more often produced forwards than the W^-, and we therefore expect an excess of positive dileptons over negative ones in the proton direction. The analysis of this type of signal requires a very careful study of the final state but may provide information on the decay modes of the weak bosons which is not obtainable otherwise.

5.4. Pair Production of Weak Bosons

One of the fundamental properties of the gauge model of electroweak interactions is the presence of bilinear couplings among gauge bosons like WWZ and WWγ, as shown in section I. These couplings allow one to produce (Brown & Mikaelian 1979, Brown et al 1979) pairs of weak bosons W^+W^-, $W^\pm Z^0$, $W^\pm\gamma$. As in the case of e^+e^- annihillation pair production of weak bosons can tell us about the gauge structure and the relevance of the renormalizability of physical theories. It would be particularly interesting to compare the W^+W^-, $W^\pm Z^0$ and Z^0Z^0 cross- sections and their dependences on the invariant

masses of the boson pairs. At energy colliders with $\sqrt{s}$ ~ 500-2000 GeV the expected cross-sections are at the picobarn level (10^{-36} cm ^{2}), and in addition the final state analysis can be complicated because of the leptons or hadronic jets. A final state with a higher cross-section is $W^{\pm}\gamma$, which directly probes the WWγ coupling and can give a measure of the anomalous moment κ of the W, whose gauge theory value is -1. This process may be seen earlier because of a larger rate and the relatively easy indentification of a large transverse momentum photon.

Table 3: Comparison of hadron-hadron colliding beam projects

Name	Location	Maximum center-of-mass energy (GeV)	Expected luminosity ($cm^{-2}sec^{-1}$)	Status
$\bar{p}p$ collider	CERN, Switz.	540	10^{30}	In operation
ISABELLE (pp)	Brookhaven, USA	800	10^{32}	Under construction
Tevatron I($\bar{p}p$)	FNAL, USA	2000	10^{30}	Approved

VI. HIGGS BOSONS

While the main subjects of this review are the intermediate vector bosons $W^{\pm}$ and Z^0, for completeness we also add here at the end a few remarks about Higgs bosons. We saw in section I how in the "standard" SU(2) × U(1) model the vector bosons acquire their masses through the vacuum expectation value of complex isodoublet Higgs field, and how one linear combination H (1.30) of electrically neutral components survives the mass generation mechanism to remain as a physical Higgs particle. In more complicated versions of the theory there are more physical Higgs particles, including charged states as well as neutrals. Many physicists find Higgs fields inelegant, and would like to replace elementary spin-zero fields by composites made out of elementary fermions (Beg & Sirlin 1974, Farhi & Susskind 1981). We do not have space here to describe in detail the phenomenology of either the minimal Higgs scenario or the alternatives, but limit ourselves to a few descriptive remarks.

The single physical Higgs particle in the minimal model has an unknown mass: in the notation (1.28) of section 1:

$$m_H^2 = 2\mu^2 + \text{radiative corrections} \tag{6.1}$$

where μ^2 is unknown, only the Higgs vacuum expectation value $v^2 = \frac{\mu^2}{\lambda}$ (1.29) being phenomenologically determined:

$$v = (\sqrt{2}\, G_F)^{-1/2} \tag{6.2}$$

The radiative corrections to the Higgs boson mass are significant (Coleman & Weinberg 1973) for small values of μ^2, and give a lower

bound to m_H corresponding to the case $\mu^2 = 0$:

$$m_H^2 = \frac{3\alpha^2}{8\sqrt{2}\, G_F} \left\{ \frac{2 + \sec^4\theta_w}{\sin^4\theta_w} - O\left(\frac{m_f}{m_w}\right)^4 \right\} \tag{6.3}$$

The experimental value of $\sin^2\theta_w$ leads to a lower bound on the Higgs boson mass of order 10 GeV. Larger masses correspond to larger values of the Higgs self-coupling (1.28), which becomes strong (Lee et al 1977, Veltman 1977) unless $m_H < O(1)$TeV. One may therefore expect the Higgs boson mass to be within an order of magnitude of the $W^{\pm}$ and Z^0 masses.

In contrast to its mass, the couplings of the minimal Higgs particle are completely determined. The couplings to the $W^{\pm}$ and Z^0 are given in equation (1.33), while since the Higgs vacuum expectation value gives masses to all the fundamental fermions f,

$$g_{H\bar{f}f} = \frac{m_f}{v} = (\sqrt{2}\, G_F)^{1/2} m_f \tag{6.4}$$

We see from equations (1.33) and (6.4) that the Higgs particle likes to couple to heavy particles such as the top quark, the $W^{\pm}$ and the Z^0, and these provide the most favorable production mechanisms.

If the Higgs boson weighs significantly less than twice the mass of the top quark, a good place to look for the Higgs boson is in $^3S_1$ toponium decay, where it has been calculated (Wilczek 1977) that

$$\frac{\Gamma(^3S_1(\bar{t}t) \to H + \gamma)}{\Gamma(^3S_1(\bar{t}t) \to \gamma^* \to e^+e^-)} \approx \frac{G_F m_t^2}{\sqrt{2}\pi\alpha} \tag{6.5}$$

This ratio is $\gtrsim 10\%$ for a top quark of mass $\gtrsim 18$ GeV, the lower limit established by the non-observation of the top quark at PETRA. When toponium is found, the Higgs boson should be one to the first objects looked for in its decays. Other good mechanisms for producing the Higgs boson involve the Z^0. Figure 22 shows the branching ratios relative to Z^0 decay into e^+e^- or $\mu^+\mu^-$ of the decays $Z^0 \to H + (e^+e^- \text{or } \mu^+\mu^-)$ (Bjorken 1977) and $Z^0 \to H + \gamma$ (Cahn et al 1979). The branching ratios for both decays are greater than 10^{-6} if $m_H \lesssim 50$ GeV, so that the Higgs boson may be visible in e^+e^- experiments with the expected ten million Z^0 decays. Another good way (Ellis et al 1976, Lee et al 1977) to produce the Higgs boson is in association with the Z^0 though the reaction $e^+e^- \to Z^0 \to Z^0 + H$ shown in figure 23. This has a cross-section

$$\frac{\sigma(e^+e^- \to Z^0 + H)}{\sigma(e^+e^- \to \mu^+\mu^-)} \gtrsim 0.1 \qquad (6.6)$$

for $m_H < 100$ GeV at a center-of-mass energy of 200 GeV. Thus a high energy e^+e^- machine such as LEP should (Camilleri et al 1976) be able to see a neutral Higgs boson with a mass up to O(100)GeV.

The charged Higgs bosons expected in more complicated theories can be pair-produced in e^+e^- annihilation, and may also be the dominant decay products of heavier quarks and leptons. Their couplings to other particles are generally correlated with their masses, but this connection is not as clear-cut as it is in the minimal model with just one neutral Higgs boson. While theories of dynamical symmetry breaking avoid the introduction of fundamental spin-zero fields,

they nevertheless tend to predict many light composite spin-zero bosons with properties analogous to Higgs particles (Bég & Sirlin 1974, Farhi & Susskind 1981). Thus they can be searched for in many of the reactions previously mentioned in connection with Higgs bosons. However, an important difference is that one does not expect (Ellis et al 1981) large couplings to the $W^{\pm}$ and Z^{0}, and so copious production of composite spin-zero bosons in association with the intermediate vector bosons is not to be expected.

VII. CONCLUSIONS

In this review we have shown how the phenomenological successes of gauge theories of the weak and electromagnetic interactions motivate very strongly the search for charged and neutral vector bosons with masses 0(80 to 90) GeV in the standard model. We have also seen how one can make quite precise predictions for the masses, decay and production cross-sections for these vector bosons in e^+e^-, lepton-hadron and hadron-hadron collisions. These three different types of experiment are largely complimentary in the information they may provide about the vector bosons and their couplings. Electron-positron collisions will not produce very heavy vector bosons in the near future, but can provide us with very detailed information about the Z^0 and provide the best prospects for searching for scalar bosons. Lepton-hadron collisions can provide indirect evidence even for rather heavy vector bosons, but are not the best types of collision to product them directly. Hadron-hadron collisions can produce even rather heavy vector bosons because of the very high center-of-mass energies they provide, but the complicated nature of the hadronic final states will make it difficult to determine their detailed properties. Hadron-hadron colliders which should be able to produce the $W^{\pm}$ and Z^0 are in operation and under construction, while one e^+e^- machine capable of producing the Z^0 has been approved. Projects for detecting ultra high energy cosmic ray neutrino collisions and ep colliding rings are being proposed. There is every reason to hope that in a few years

the physics of the weak vector bosons will be thoroughly studied in many experiments. We hope and trust they will provide us with exciting surprises.

ACKNOWLEDGEMENTS

We thank the many participants in various studies of future high energy accelerator projects for enjoyable collaborations. In particular, we wish to acknowledge the LEP study contributions of P. Darriulat and F. Renard, and we especially thank C. H. Llewellyn Smith, B. Richter and B. H. Wiik for advice and encouragement. This work was supported by the Director, Office of Energy Research, Office of High Energy and Nuclear Physics, Division of High Energy Physics of the U.S. Department of Energy under Contract DE-AC03-76SF00098.

FIGURE CAPTIONS

Fig. 1. The ratio R_μ of $\sigma(e^+e^- \to \mu^+\mu^+)$ relative to σ_0 [Eq. (3.2)], plotted for different values of the vector and axial vector couplings of e and μ (radiative corrections not included).

Fig. 2. The forward backward asymmetry A_μ [Eq. (3.12)] for $e^+e^- \to \mu^+\mu^-$, plotted for axial couplings $a_e = a_\mu = 1$, and different values of the e and μ vector coupling.

Fig. 3. The cross section ratio R_μ as a function of c.m. energy in a model with two neutral vector bosons and in the standard model with m_Z=94 GeV and $\sin^2\theta_w$=0.20(solid line)(deGroot et al 1979).

Fig. 4. Cross section (Alles et al 1977) for $e^+e^- \to W^+W^-$ for different values of the weak neutral current angle in the standard model.

Fig. 5. Contributions σ_{aa} from pure a exchange and σ_{ab} from a, b exchange interference to the cross section for $e^+e^- \to W^+W^-$ calculated (Alles et al 1977) in the standard model using $\sin^2\theta_w = 3/8$.

Fig. 6. Energy dependence of the angular projection of the contribution to $\sigma(e^+e^- \to W^+W^-)$ from interference between direct-channel vector exchange and cross channel neutrino exchange for (a) photon and ν exchange only, (b) the standard model with $\sin^2\theta_w = 0.25$ and (c) the standard model including an (e_R^-, ν_R) weak doublet. Error bars represent a typical LEP experiment with a leptonic W-decay trigger.

Fig. 7. The ratio between up coming and down coming muons from ultra high energy cosmic ray neutrino interactions is sensitive to the amount of absorption of neutrinos passing through the Earth. The ratio would be unity in the absence of absorption, while a linearly rising neutrino cross-section (corresponding to $m_W \gg 80$ GeV) entails more absorption than the slower-rising cross-section found if $m_W = 80$ GeV. The error bars indicate the experimental results which would be obtained from DUMAND (1982).

Fig. 8. Rate of events per day expected at HERA for $e^- + p \rightarrow \nu + X$ in Q^2 bins of 5000 GeV^2.

Fig. 9. The ratios between the cross-sections for left-and right-handed electron-proton scattering at a center-of-mass $(\text{energy})^2 = 27{,}000\ GeV^2$, for different values of the Z^0 mass: x and y are the standard kinematical variables (Barish 1978) for lepton-nucleon scattering.

Fig. 10. Feynman diagrams for direct production of weak vector bosons in lepton-hadron collisions: (a) for $W^{\pm}$ production from the leptonic vertex, (b) for Z^0 production from the leptonic vertex, (c) for $W^{\pm}$ or Z^0 production from the hadronic vertex.

Fig. 11. The cross-section for Z^0 and $W^{\pm}$ production at the leptonic vertex estimated by scaling up low energy results. These events are generally relatively clean, with either a proton or a simple hadronic system accompanying the

vector boson. Events where the production takes place at the hadronic vertex are likely to contain a much more complicated hadronic system.

Fig. 12. The original Drell-Yan mechanism.

Fig. 13. Kinematics of weak boson (W) production.

Fig. 14. First order QCD contributions to W production.

Fig. 15. Evolution of the valence quark (u,d) distributions with Q^2.

Fig. 16. Predicted production cross sections for W and Z^0 in pp and $p\bar{p}$ collisions. The calculated cross-sections include scale breaking effects (Paige 1979).

Fig. 17. Lepton pair mass spectrum in $p\bar{p}$ collisions at $\sqrt{s}$ = 540 GeV.

Fig. 18. The Jacobian peak of the single lepton spectrum from W^+ production and decay. The calculation is indicated by "DY", while "QCD" contains the QCD corrections (Aurenche & Lindfors 1981 a,b).

Fig. 19. Schematic description of the helicity configuration in the reaction $p\bar{p} \rightarrow W^+ \rightarrow \ell^+ \nu_\ell$. Single (double) arrows indicates the momentum (helicity) direction.

Fig. 20 The front back W^- asymmetry a) versus $\cos\theta$ for various values of $\sqrt{\tau}$, b) integrated version as a function of $1/\sqrt{\tau}$ (Perrottet 1978, Finjord et al 1981).

Fig. 21 Invariant mass spectrum of heavy quark pairs from W,Z and gluon fusion. The mass of the top quark is chosen as 30 GeV/c.

Fig. 22. Branching ratios relative to $Z^0 \to \mu^+\mu^-$ for $Z^0 \to H^0\mu^+\mu^-$ and $Z^0 \to H + \gamma$.

Fig. 23. Lowest order Feynman diagram for the process $e^+e^- \to Z^0 + H$.

REFERENCES

Abbott, L. F., Farhi, E. 1981, Nucl. Phys. B180: 547-

Abud, M., Gatto, R., Savoy, C. A. 1978. Phys. Lett. 79B: 435-

Abud, M., Gatto, R., Savoy, C. A. 1979. Phys. Rev. D20: 1164-

Albert, D., Marciano, W. J., Wyler, D., Parsa, Z. 1980, Nucl. Phys. B119: 125-

Alles, W., Boyer, C., Buras, A. J. 1977. Nucl. Phys. B119: 125-

Altarelli, G., Ellis, R. K., Martinelli, G. 1979 Nucl. Phys. B147: 461-

Amaldi, U. ed. 1980. Possibilities and Limitations of Accelerators and Detectors. Proceedings, 2nd ICFA workshop, Les Diablerets, Switzerland, 4-10 October 1979. Geneva, Switzerland: CERN, Publ. Group 1980 442p.

Asano, Y., Kikutani, E., Kurokawa, S., Miyachi, T., Miyajima, M., Nasashima, Y., Shinkawa, T., Susimoto, S., Yoshimura, Y., KEK Preprint -81-17 1981. Submitted to Phys. Lett.

Aubert, J. J., Becker, U., Biggs, P. J., Burger, J., Chen M., Eerhart, G., Goldhagen, P., Leong, J., McCorrison, T., Rhoades, T. G., Rohde, M., Ting, S. C. C., Wu, Sau Lan, Lee, Y. Y. 1974: Phys. Rev. Lett. 33: 1404-

Augustin, J. -E., Boyarski, A. M., Breidenbach, M., Bulos, F., Dakin, J. T., Feldman, G. J., Fischer, G. E., Fryberger, D., Hanson, G., Jean-Marie, B., Larsen, R. R., Luth, V., Lynch, H. L., Lyon, D., Morehouse, C. C., Paterson, J. M., Perl, M. L., Richter, B., Rapidis, P., Schwitters, R. F.,

Tanenbaum, W. M., Vannucci, F., Abrams, G. S., Briggs, D., Chinowsky, W., Friedberg, C. E., Goldhaber, G., Hollenbeek, R. J., Kadyk, J. A., Lulu, B., Pierre, F., Trilling, G. H., Whitaker, J. S., Wiss, J., Zipse, J. E., 1974. Phys. Rev. Lett. 33: 1406-

Aurenche, P., Lindfors, J., 1981 a. Nucl. Phys. B185: 274-

Aurenche, P., Lindfors, J., 1981 b. Nucl. Phys. B185: 301-

Bardin, D. Yu., Dokuchaeva, V. A. 1981. On Radiative Corrections To neutrino N → neutrino X Process. (In Russian), JINR-P2-81-552, Submitted to Yadernaya Fiz.

Barish, B., 1978. Phys. Rep. 39: 279.

Bèg, M. A. B., Sirlin, A. 1974. Ann. Rev. Nucl. Sci. 24: 379-

Bjorken, J. D. 1977. Proc. 1974 SLAC Summer Institute of Particle Physics (SLAC-198).

Bollini, D., Frabetti, P. L., Heiman, G., Monari, L., Navarria, F. L., Benvenutti, A. C., Bozzo, M., Brun, R., Gennow, M., Goossens, M., Kopp, R., Navach, F., Piemontese, L., Pilcher, J., Schinzer, D., Bardin, D. Yu., Cvach, J., Fadeev, N. G., Golutvin, I. A., Kiryushin, Y. T., Kisselev, V. S., Klein, M., Krivokhizhin, V. G., Kukhtin, V. V., Nowak, W. D., Savin, I. A., Smirnov, G. I., Vesztersombi, G., Volodko, A. G., Zacek, J., Jamnik, D., Meyer-Berkhout, U., Staude, A., Teichert, K. M., Tirler, R., Voss, R., Zupancic, C., Dobrowolski, T., Feltesse, J., Maillard J., Malasoma, J. M., Milsztajn, A., Renardy, J. F., Sacquin, Y., Smadja, G., Verrecchia, P., Virchaux, M. 1982. Paper to be published.

Branson, J. G. 1981. Recent Experimental Tests of the Electroweak Theory. DESY 81/073, To be published in Proc. 10th Int. Symp. on

Lepton and Photon Interactions at High Energy, Bonn, West Germany, Aug. 24-29, 1981.

Brown, R. W., Mikaelian, K. O. 1979. Phys. Rev. D19: 922-

Brown, R. W., Sahdev, D., Mikaelian, K. O. 1979. Phys. Rev. D20: 1164-

Cabibbo, N. 1963. Phys. Rev. Letters 10: 531

Cahn, R. N., Chanowitz, M. S., Fleishon, N. 1979. Phys. Lett. 82B: 113-

Camilleri, L., Cundy, D., Darriulat, P., Ellis, J., Field, J., Fischer, H., Gabathuler, E., Gaillard, M. K., Hoffmann, H., Johnsen, K., Keil, E., Palmonari, R., Preparata, G., Richter, B., Rubbia, C., Steinberger, J., Wiik, B., Willis, W., Winter, K., 1976. Physics with very high energy e^+e^- colliding beams. CERN 76-18.

Coleman, S., Weinberg, E., 1973. Phys. Rev. D7: 1888-

Danby, G., Gaillard, J. -M., Goulianos, D., Lederman, L. M., Mistry, N., Schwartz, M., Steinberger, J. 1962. Phys. Rev. Lett. 9: 36

de Groot, E. H., Gounaris, G. J., Schildknect, D. 1979. Phys. Lett. 85B: 399-

Drell, S. D., Yan, T. H. 1971. Ann. Phys. NY 66: 578.

DUMAND 1982. Project Description prepared by the Hawaii Dumand Center.

ECFA, CERN 1979. Proc. LEP Summer Study, Les Houches and CERN, Sept. 1978, CERN 79-01. Vols. 1, 2.

ECFA, DESY 1979. Proceedings of an ep facility for Europe, DESY 79/48.

Ellis, J. 1981. Lectures presented at the 1981 Les Houches Summer School, LAPP preprint TH-48/CERN TH-3174.

Ellis, J., Gaillard, M. K., Nanopoulos, D. V. 1976. Nucl. Phys. B106: 292-

Ellis, J., Gaillard, M. K., Nanopoulos, D. V., Sikivie, P. 1981. Nucl. Phys. B182: 529

Nucl. Phys. B182: 529-45.

Ellis, J., et al. 1978. CHEEP: An ep Facility in the SPS. CHEEP Study Groups CERN 78-02.

Farhi, E., Susskind, L. 1981. Phys. Rep. 74C: 277-

Fermi 1933. La Ricerca Scientifica 4: 491

Feynman, R. P. 1972. Photon Hadron Interactions. Reading, Mass. Benjamin.

Finjord, J., Girardi, G., Perrottet, M., Sorba,P. 1981. Nucl. Phys. B182: 427-

Gaemers, D. J. F., Gounaris, G. J. 1979. Z. Phys. C1: 259

Gaillard, M. K., Lee, B. W. 1974. Phys. Rev. D10: 897-

Gell-Mann, M., Levy, M. 1960. Nuovo Cimento 16: 705

Georgi, H., Glashow, S. L. 1972. Phys. Rev. Lett. 28: 1494

George, H., Weinberg, S. 1978. Phys. Rev. D17: 275

Glashow, S. L. 1961. Nucl. Phys. 22: 579-

Glashow, S. L., Iliopoulos, J., Maiani, L. 1970. Phys. Rev. D2: 1285-

Goldhaber, G., Pierre, F. M., Abrams, G. S., Alam, M. S., Boyarski, A. M., Breidenbach, M., Carithers, W. C., Chinowsky, W., Cooper, S. C., DeVoe, R. G., Dorfan, J. M., Feldman, G. J., Friedberg, C. E., Fryberger, D., Hanson, G., Jaros, J., Johnson, A. D., Kadyk, J. A., Larsen, R. R., Lüke, D., Lüth, V., Lynch, H. L., Madaras, R. J., Morehouse, C. C., Nguyen, H. K., Paterson, J. M., Perl. M. L., Peruzzi, I., Piccolo, M., Pun, T. P., Rapidis, P., Richter, B., Sadoulet, B., Schindler, R. H., Schwitters, R. F., Siegrist, J., Tanenbaun, W., Trilling, G. H., Vannucci, F., Whitaker, J., Wiss, J. E. 1976. Phys. Rev. Letters 37 255-

Goldstone, J. 1961. Nuov. Cim. 19: 564

Hasert, F. J., Kabe, S., Krenz, W., Von Krogh, J., Lanske, D., Morfin, J., Schultze, K., Weerts, H., Bertrand-Coremans, G. H., Sacton, J., Van Doninck, W., Vilain, P., Camerini, U., Cundy, D. C., Baldi, R., Danilchenko, I., Fry, W. F., Haidt, D., Natali, S., Musset, P., Osculati, B., Palmer, R., Pattison, J. B. M., Perkins, D. H., Pullia, A., Rousset, A., Venus, W., Wachsmuth, H., Brisson, V., Degrange, B., Haguenauer, M., Kluberg, L., Nguyen-Khan, U., Petiau, P., Belotti, E., Bonetti, S., Cavalli, D., Conta, C., Fiorini, E., Rollier, M., Aubert, B., Blum, D., Chounet, L. M., Heusse, P., Lagarrigue, A., Lutz, A. M., Orkin-Lecourtois, A., Vialle, J. P., Bullock, F. W., Esten, M. J., Jones, T. W., McKenzie, J., Michette, A. G., Myatt, G., Scott, W. G. 1973. Phys. Lett. 46B: 138

Herb, S. Hom, D. C., Lederman, L. M. Sens, J. C. Snyder, H. D., Yoh, J. K., Appel, J. A., Brown, B. C.,Brown, C. N. Innes, W. R., Ueno, K., Yamanouchi, T., Ito. A. S., Jöstlein, H., Kaplan, D. M., Kephart, R. D. 1977. Phys. Rev. Lett. 39: 252-

Higgs, P. W. 1964. Phys. Lett. 12: 132

Humpert, B., van Neerven, W. L. 1980. Phys. Lett. 93B: 456

Hung, P. W., Sakurai, J. J. 1981. Ann. Rev. Nucl. Part. Sci. 31: 375-

Kamal, A. N., Ng, J. N., Lee, H. C. 1981. TRIUMF and University of Alberta preprint TRI-PP-81-15/Alberta thy-8-91. Submitted to Phys. Rev. D.

Kibble, T. W. B. 1967. Phys. Rev. 155: 1554

Kobayashi, M., Maskawa, K. 1973. Prog. Theor. Phys. 49: 652-

Lee, B.W. 1972. Phys. Rev. D6: 1188

Lee, B. W., Quigg, C., Thacker, H. B. 1977. Phys. Rev. D16: 1519-

Lee, B. W., Zinn-Justin, J. 1972. Phys. Rev. D5: 3121, 3137, 3155.

Llewellyn Smith, C. H, Wheater, J. 1981. Phys. Lett. 105B: 486

Llewellyn Smith, C. H., Wiik, B. 1977. DESY preporнt 77/38 (unpublished).

Marciano, W., Parsa, Z. 1981. Proc. Cornell Z^0 Theory Workshop, ed. Peskin, M. E., and Tye, S. -H. H. CLNS 81-485, p. 127

Paige, F. 1979. Proc. Topical Workshop on the Production of New Particles in Super High Energy Collisions, ed. V. Barger and F. Halzen (Univ. of Wisconsin, Madison, 1979).

Pakvasa, S., Dechantsreiter, M., Halzen F., Scott, D. M. 1979. Phys. Ref. D20: 2862

Peierls, R. F., Trueman, T. L., Wang, L. L. 1977. Phys. Rev. D16: 1397

Perl, M., Abrams, G. S., Boyarski, A. M., Breidenbach, M., Briggs, D. D., Bulos, F., Chinowsky, W., Dakin, J. T., Feldman, G. J., Friedberg, D., Fryberger, D., Goldhaber, G., Hanson, G., Heile, F. B., Jean-Marie, B., Kadyk, J. A., Larsen, R. R., Litke, A. M., Lüke, D., Lulu, B. A., Lüth, V., Lyon, D., Morehouse, C. C., Paterson, J. M., Pierre, F. M., Pun, T. P., Rapidis, P. A., Richter, B., Sadoulet, B., Schwitters, R. F., Tanenbaum, W., Trilling, G. H., Vannucci, F., Whitaker, J. S., Winkelmann, F. C., and Wiss, J. E. 1975. Phys. Rev. Lett. 35: 1489-

Perrottet, M. 1978. Ann. Phys. NY 115: 107

Perruzi, I. Piccolo, M., Feldman, G. J., Locomte, P., Vuillemin, V., Barbaro-Galtieri, A., Dorfan, J. M., Ely, R., Feller, J. M.,

Fong, A., Gobbi, B., Hanson, G., Jaros, J. A., Kwan, B. P., Litke, A. M., Lüke, D., Madaras, R. J., Martin, J. F., Miller, D. H., Parker, S. I., Perl, M. L., Pun, P. T., Rapidis, P. A., Ronan, M. T., Ross, R. R., Scharre, D. L., Trippe, T. G., Yount, D. E. 1977. Phys. Rev. Lett. 39: 1301-

Peshkin, M. E., Tye, S. -H. H. Eds. 1971. Proc. Cornell Z^0 Theory Workshop. CLNS 81-485.

Prentki, J., Zumino, B. 1972. Nucl. Phys. B47: 99

Prescott, C. Y., Atwood, W. B., Cottrell, R. L. A., DeStaebler, H., Garwin, E. L., Gonidec, A., Miller, R. H., Rochester, L. S., Sato, T., Sherden, D. J., Sinclair, C. K., Stein, S., Taylor, R. E., Clendenin, J. E., Hughes, V. W., Sasao, N, Schüler, K. P., Borghini, M. G. Lübelsmeyer, K., and Jentscheke, W. 1978. Phys. Lett. 77B: 247-

Quigg, C. 1977. Rev. Mod. Phys. 49: 297

Reya, E. 1981. Phys. Rev. 69: 195

Salam, A. 1968. Proc. 8th Nobel Symposium, Stockholm 1968, ed. N. Svartholm (Almquist and Wiksells, Stockholm, 1968). p. 367.

Sirlin, A., Marciano, W. S. 1981. Nucl. Phys. B189: 442

Steigman, G. 1980. Ann. Rev. Nucl. Part. Phys.

Sushkov, O. P., Fambaum, V. V., Khriplovich, I. B. 1975. Sov. J. Nucl. Phys. 20: 537

't Hooft, G. 1971. Nucl. Phys. B35: 167.

Vainshtein A. I., Khriplovich, I. B. 1973. JETP Lett. 18: 83

Veltman, M. 1977. Acta Physica Polonica B8: 475

Veltman, M. 1980. Phys. Lett. 91B: 95.

Wahl, H. 1981. Rapporteur Talk at the 1981 E.P.S. Int. Conf. on High Energy Physics, Lisbon, to be published in the proceedings.

Weinberg, S. 1967. Phys. Rev. Lett. 19: 1264

Wilczek, F. A. 1977. Phys. Rev. Lett. 39: 1304

Yang, C. N., Mills, R. L. 1954. Phys. Rev. 96: 191

Yukawa, H. 1935, Proc. Math. Soc. Japan 17: 48

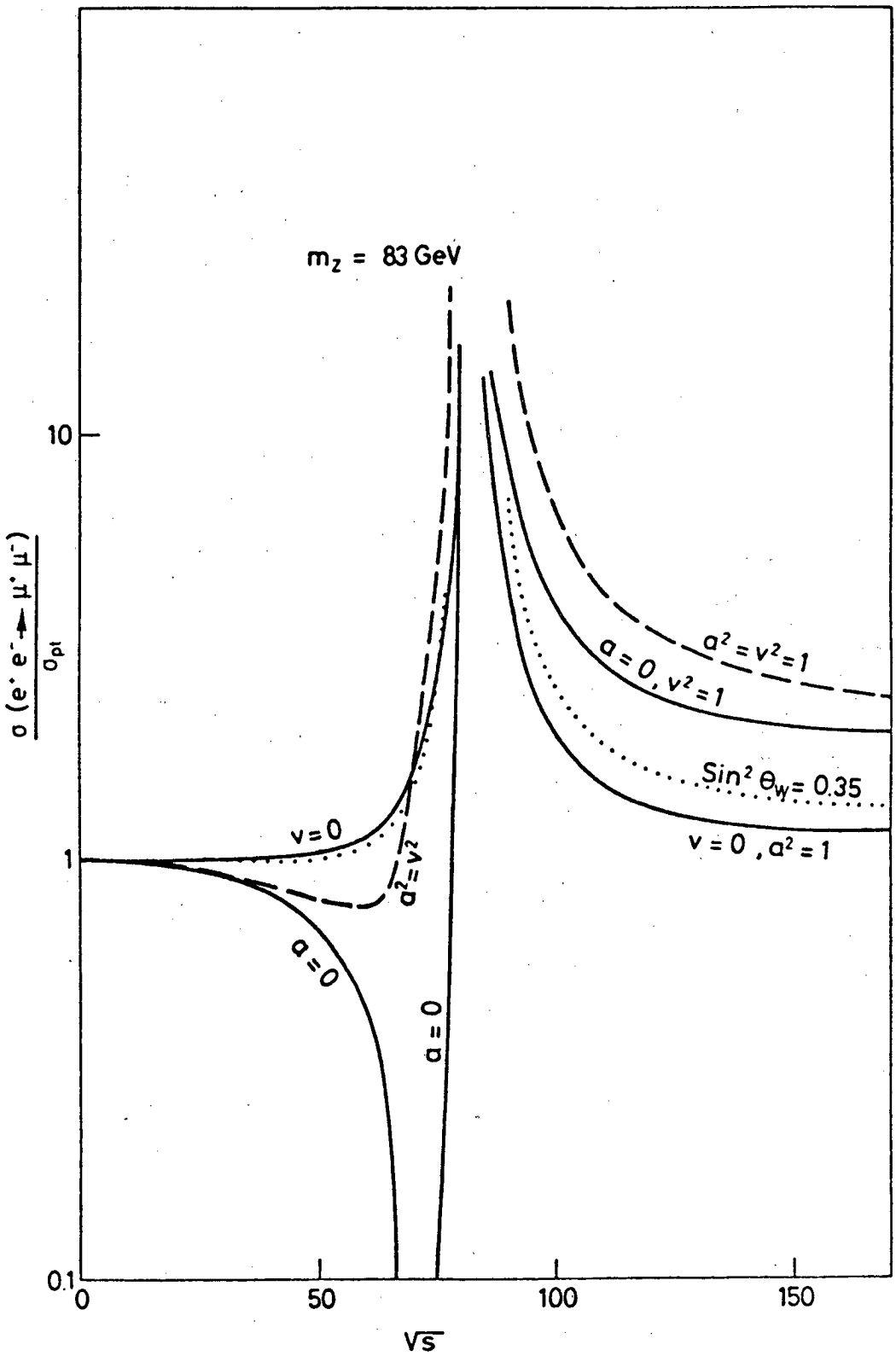
m_z = 83 GeV
$\frac{\sigma(e^+e^- \to \mu^+\mu^-)}{\sigma_{pt}}$
10
1
0.1
0
50
100
150
$\sqrt{s}$
$a^2 = v^2 = 1$
$a = 0, v^2 = 1$
$\sin^2\theta_W = 0.35$
$v = 0, a^2 = 1$
$v = 0$
$a^2 = v^2$
$a = 0$
$a = 0$

FIGURE 1

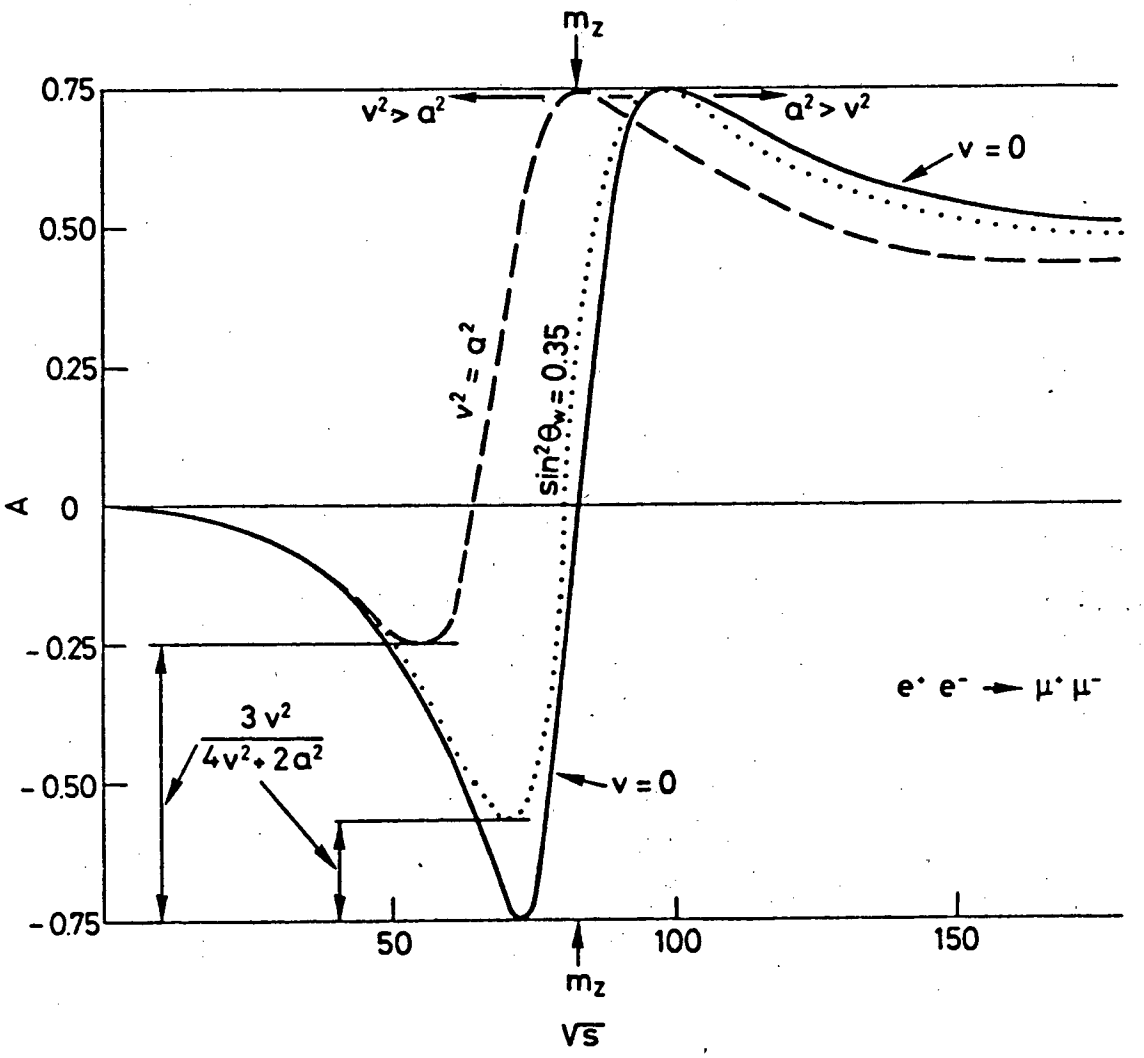
m_z
0.75
0.50
0.25
0
-0.25
-0.50
-0.75
A
$v^2 > a^2$
$a^2 > v^2$
v = 0
$v^2 = a^2$
$\sin^2\theta_w = 0.35$
$\frac{3v^2}{4v^2+2a^2}$
v = 0
$e^+ e^- \to \mu^+ \mu^-$
50
100
150
m_z
$\sqrt{s}$

FIGURE 2

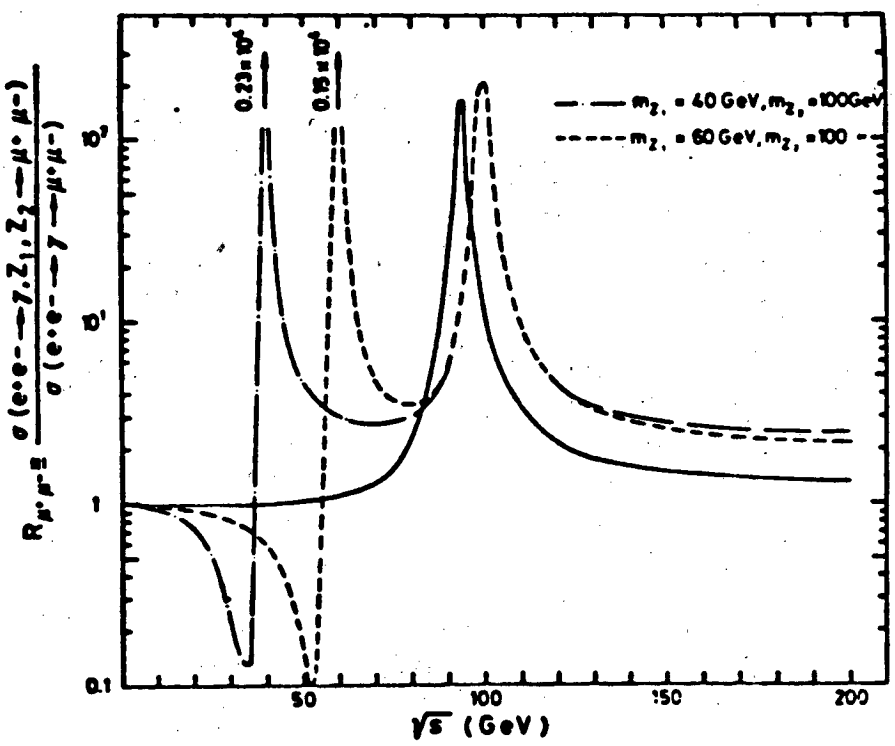
$R_{\mu^+\mu^-} \equiv \frac{\sigma(e^+e^- \to \gamma, Z_1, Z_2 \to \mu^+\mu^-)}{\sigma(e^+e^- \to \gamma \to \mu^+\mu^-)}$
0.23 GeV^{-2}
0.15 GeV^{-2}
m_{Z_1} = 40 GeV, m_{Z_2} = 100 GeV
m_{Z_1} = 60 GeV, m_{Z_2} = 100 GeV
10
1
0.1
50
100
150
200
$\sqrt{s}$ (GeV)

FIGURE 3

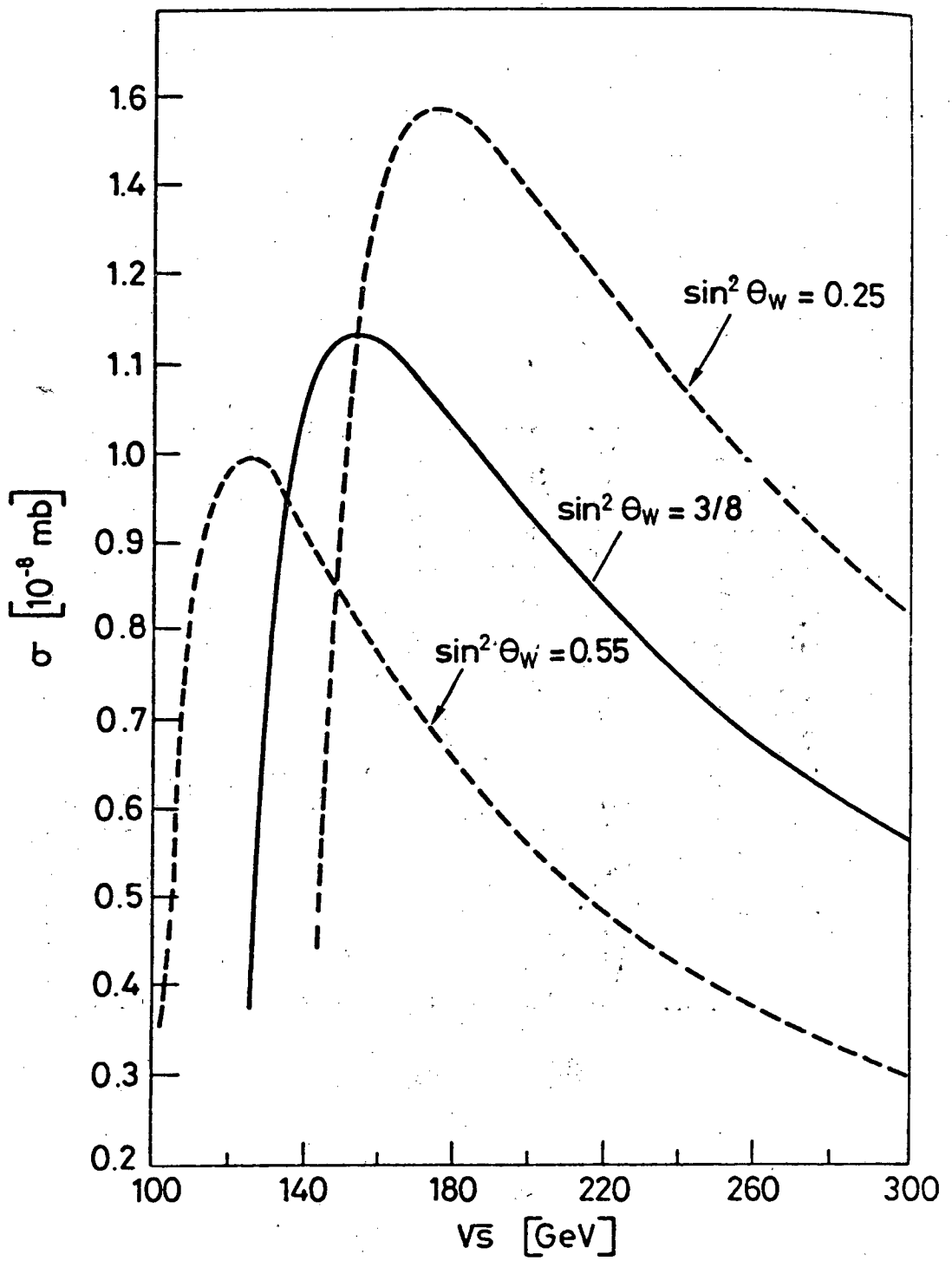
1.6
1.4
1.2
1.1
1.0
0.9
0.8
0.7
0.6
0.5
0.4
0.3
0.2
σ [10⁻⁸ mb]
sin² θW = 0.25
sin² θW = 3/8
sin² θW = 0.55
100
140
180
220
260
300
√s [GeV]

FIGURE 4

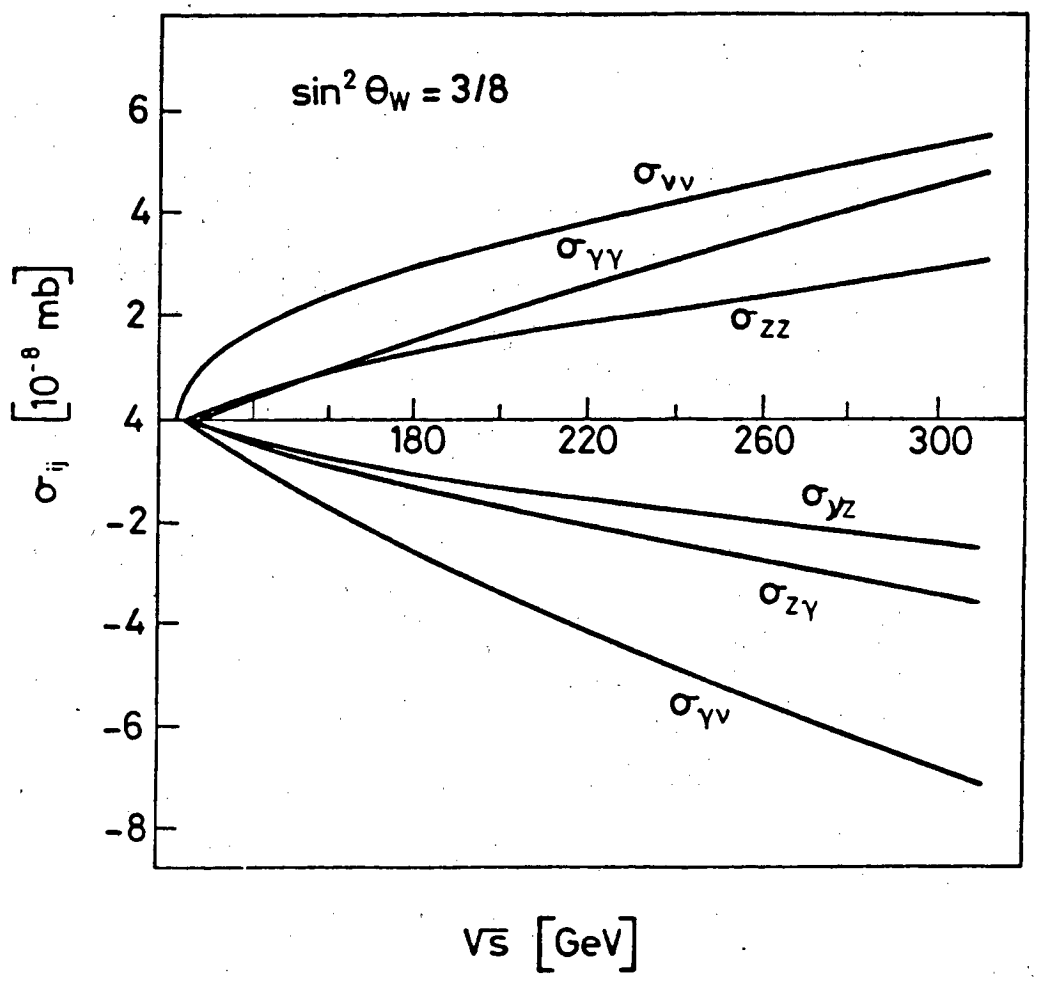
sin² θW = 3/8
σνν
σγγ
σzz
σγz
σzγ
σγν
6
4
2
4
-2
-4
-6
-8
180
220
260
300
σij [10⁻⁸ mb]
√s [GeV]

FIGURE 5

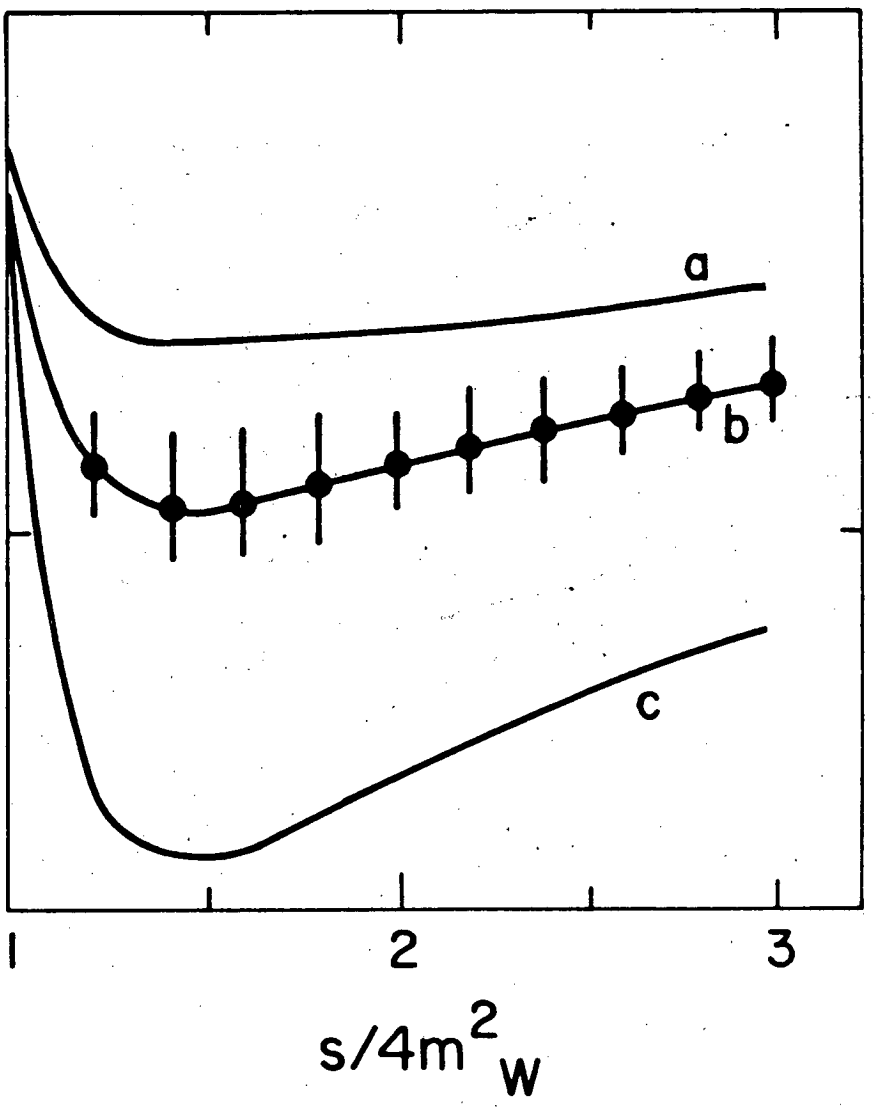

FIGURE 6 XBL 821-62

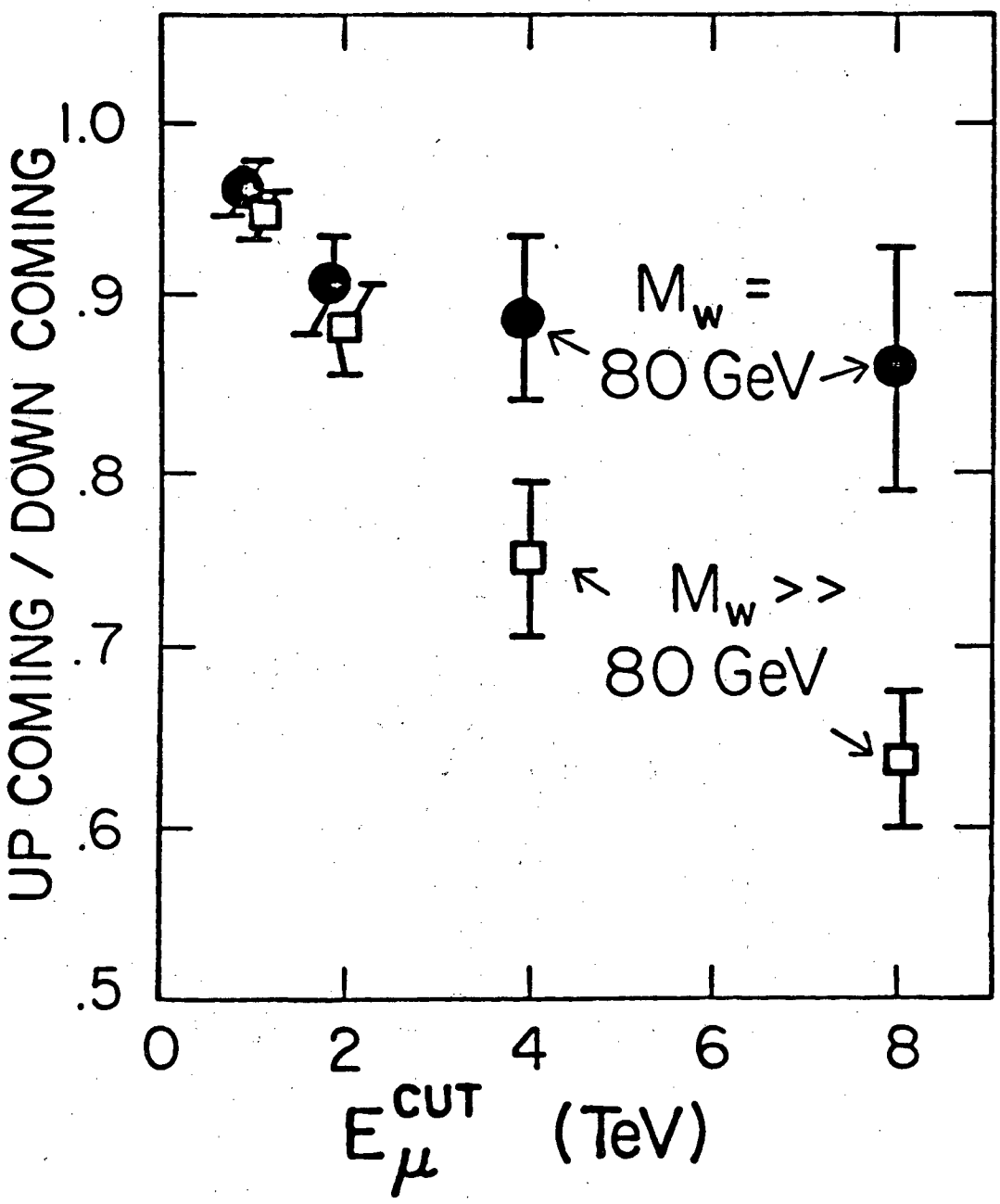
UP COMING / DOWN COMING
1.0
.9
.8
.7
.6
.5
0
2
4
6
8
E_μ^{CUT} (TeV)
M_W = 80 GeV
M_W >> 80 GeV

FIGURE 7

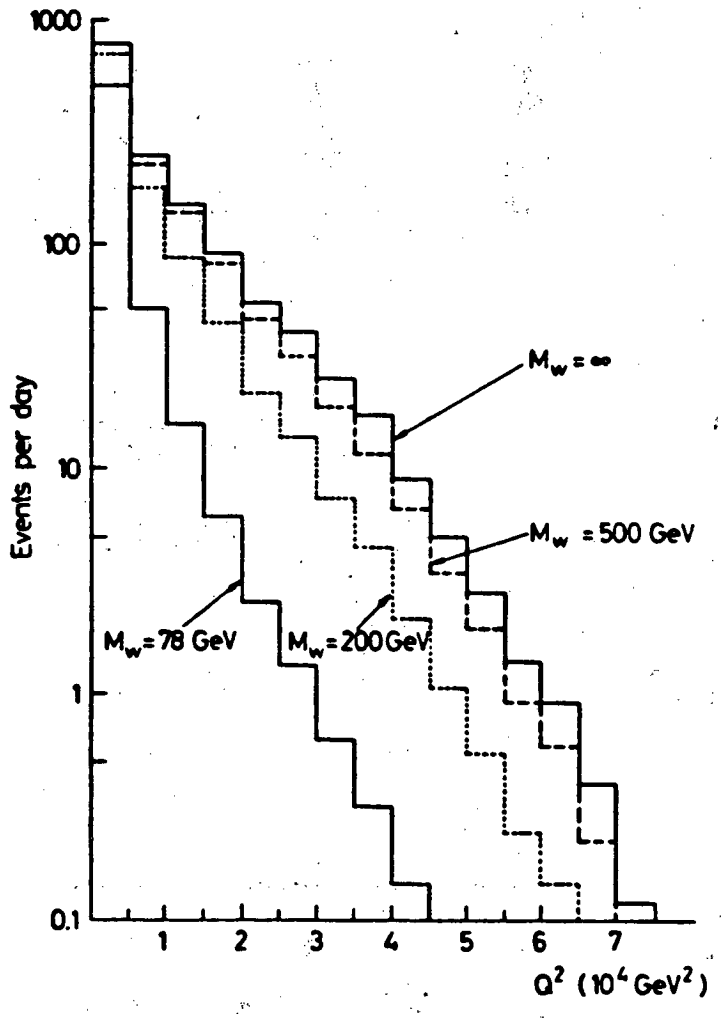
1000
100
10
1
0.1
Events per day
$M_w = \infty$
M_w = 500 GeV
M_w = 78 GeV
M_w = 200 GeV
1
2
3
4
5
6
7
Q^2 (10^4 GeV^2)

FIGURE 8

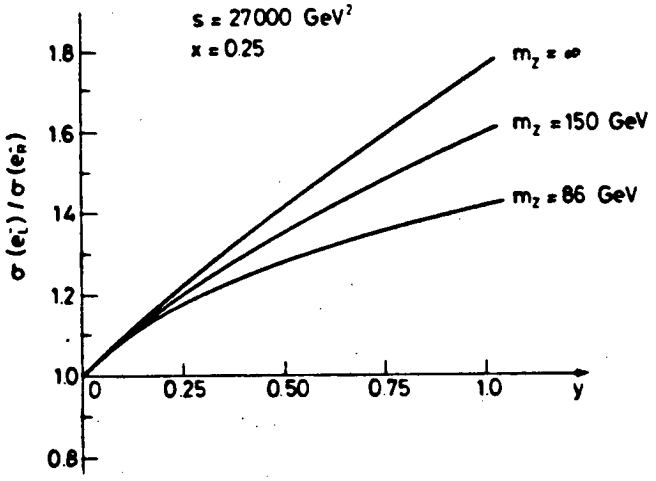
s = 27000 GeV²
x = 0.25
m_z = ∞
m_z = 150 GeV
m_z = 86 GeV
σ(e_L)/σ(e_R)
1.8
1.6
1.4
1.2
1.0
0.8
0
0.25
0.50
0.75
1.0
y

FIGURE 9

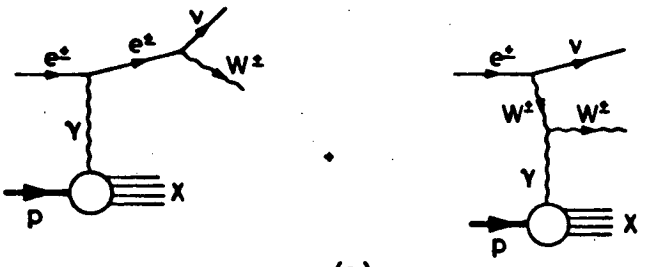

(a)

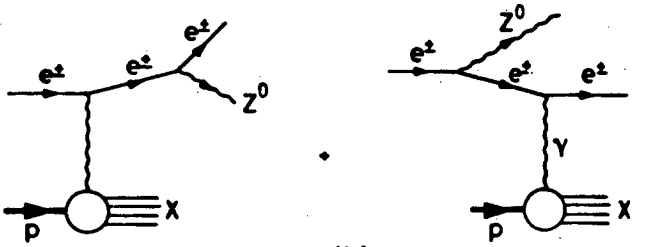

(b)

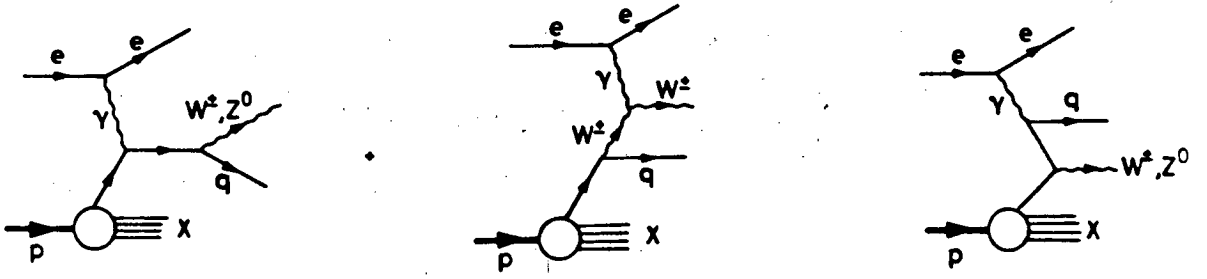

(c)

FIGURE 10

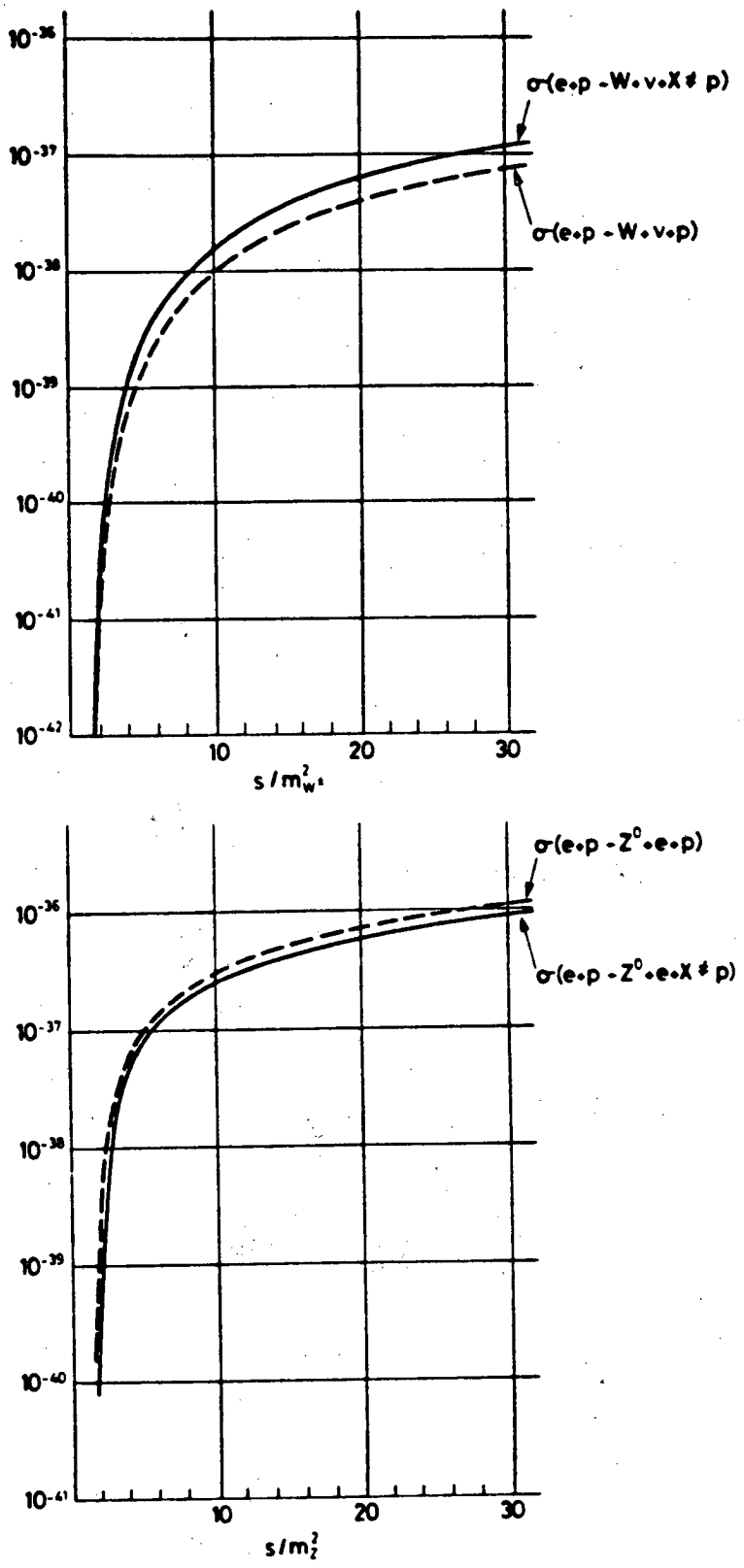
10^{-36}
10^{-37}
10^{-38}
10^{-39}
10^{-40}
10^{-41}
10^{-42}
10
20
30
$s/m^2_{W^\pm}$
$\sigma(e\cdot p \to W\cdot \nu\cdot X \neq p)$
$\sigma(e\cdot p \to W\cdot \nu\cdot p)$
10^{-36}
10^{-37}
10^{-38}
10^{-39}
10^{-40}
10^{-41}
10
20
30
s/m_z^2
$\sigma(e\cdot p \to Z^0\cdot e\cdot p)$
$\sigma(e\cdot p \to Z^0\cdot e\cdot X \neq p)$

FIGURE 11

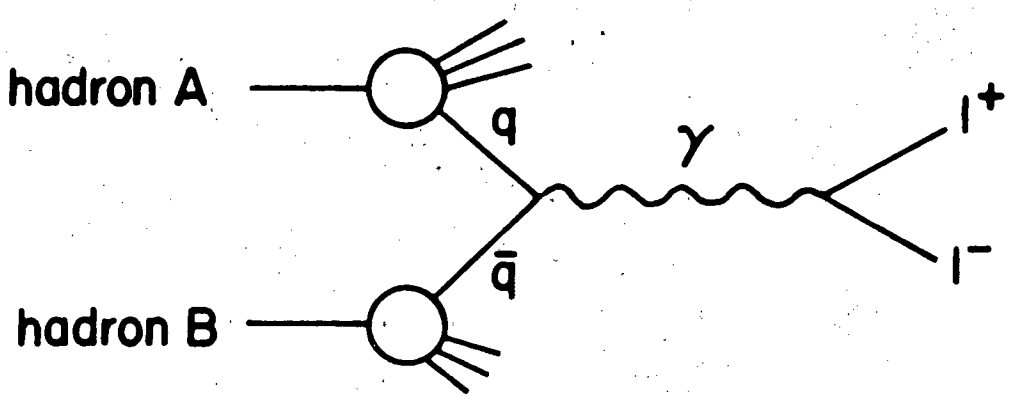

FIGURE 12

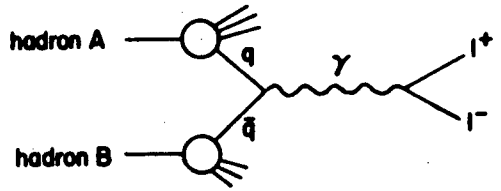

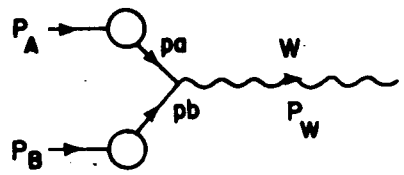

$$P_A = \left(\frac{\sqrt{s}}{2}, \vec{P}\right) \; i \; P_B = \left(\frac{\sqrt{s}}{2}, -\vec{P}\right)$$

$$Pa = x_a P_A \; i \; P_b = x_b P_B \; i P_W = \left(\frac{x_a + x_b}{2}\right)\sqrt{s} \; i \; p_\perp \sim 0 \; i P_{11} = \frac{\sqrt{s}}{2}(x_a - x_b)$$

$$\hat{s} = (p_a + p_b)^2 = x_a x_b \, s = \tau s$$

XBL 821-69

FIGURE 13

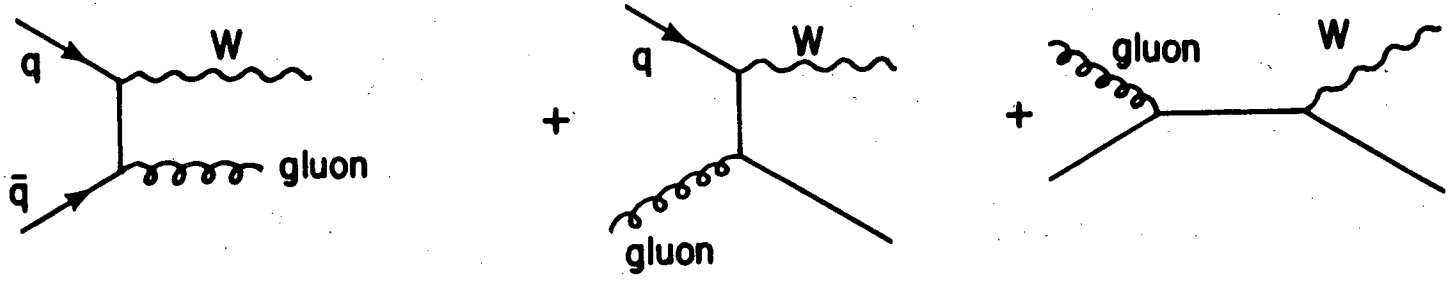

XBL 821-63

FIGURE 14

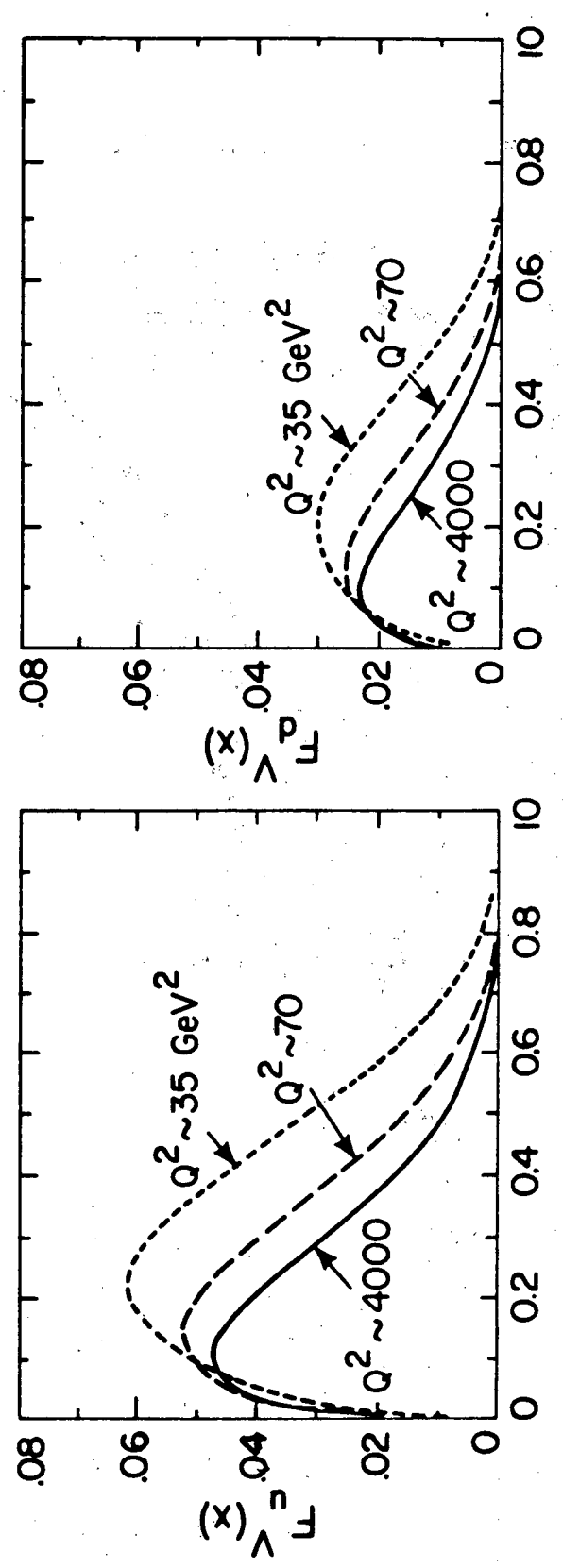
$\langle T_L^n(x) \rangle$
$\langle T_L^p(x) \rangle$
$Q^2 \sim 35$ GeV^2
$Q^2 \sim 70$
$Q^2 \sim 4000$
0
.02
.04
.06
.08
0.2
0.4
0.6
0.8
1.0
XBL 821-64

FIGURE 15

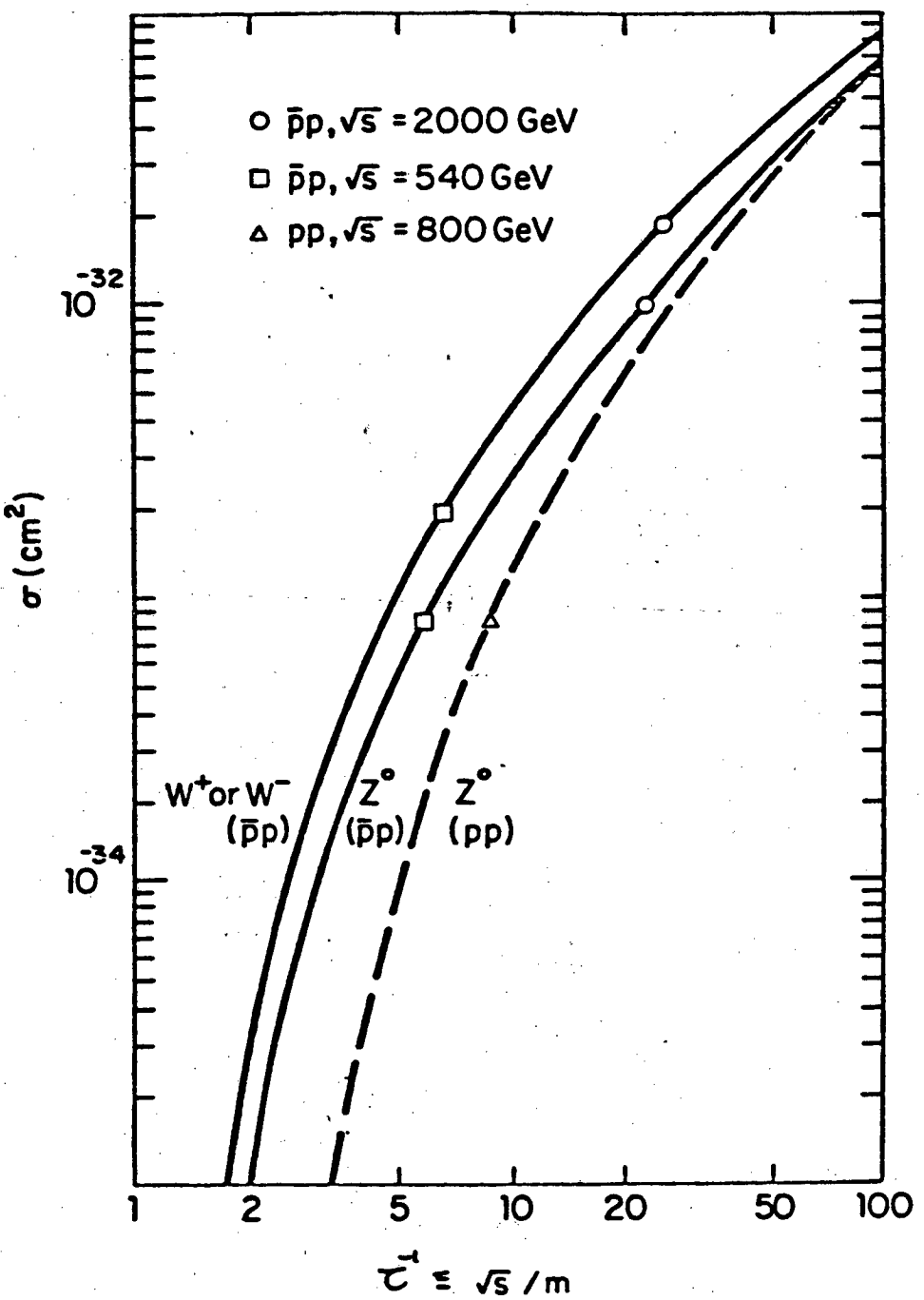
o p̄p, √s = 2000 GeV
□ p̄p, √s = 540 GeV
△ pp, √s = 800 GeV
10^-32
10^-34
σ (cm²)
W⁺ or W⁻ (p̄p)
Z° (p̄p)
Z° (pp)
1
2
5
10
20
50
100
τ⁻¹ ≡ √s / m

FIGURE 16

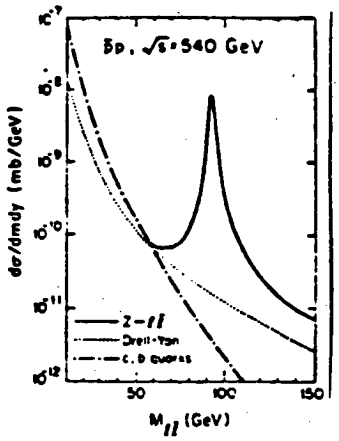

FIGURE 17

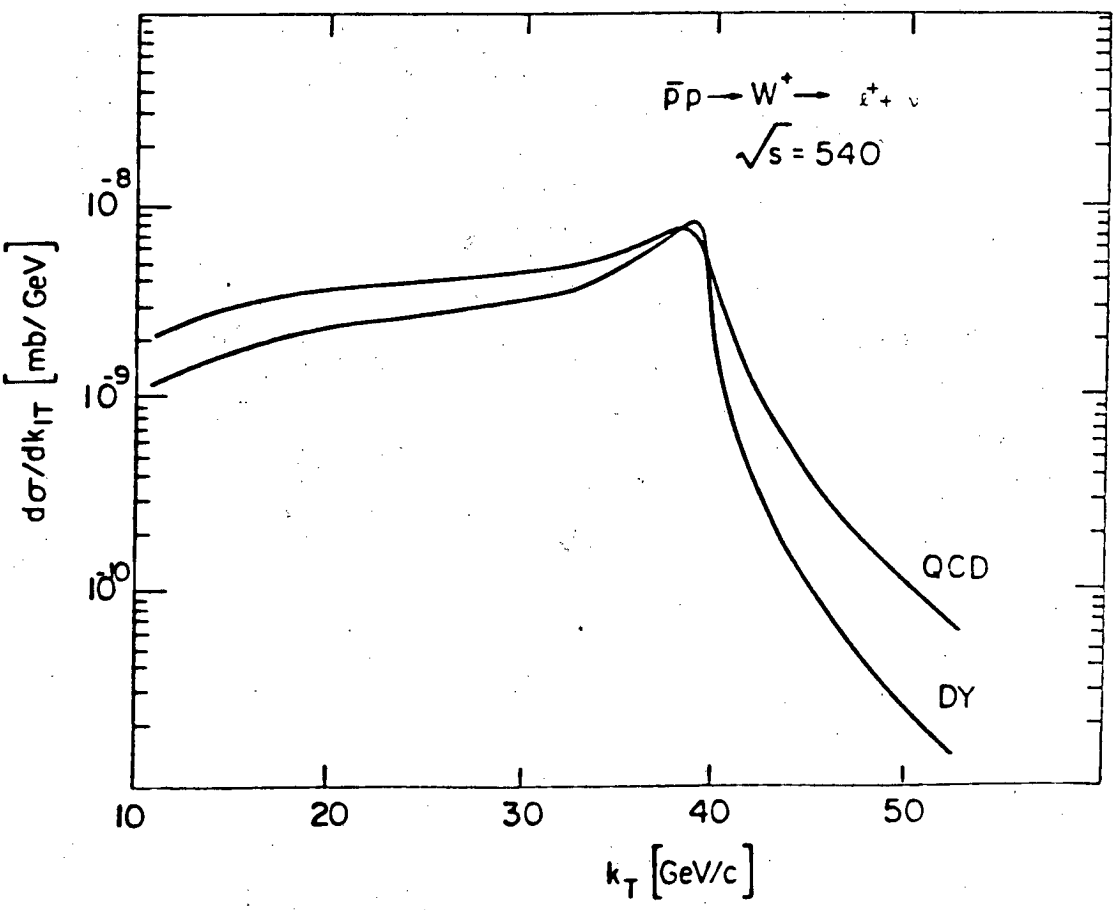

FIGURE 18

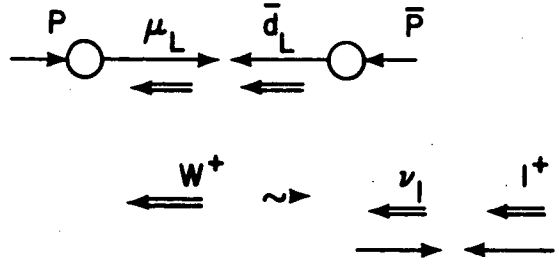

FIGURE 19

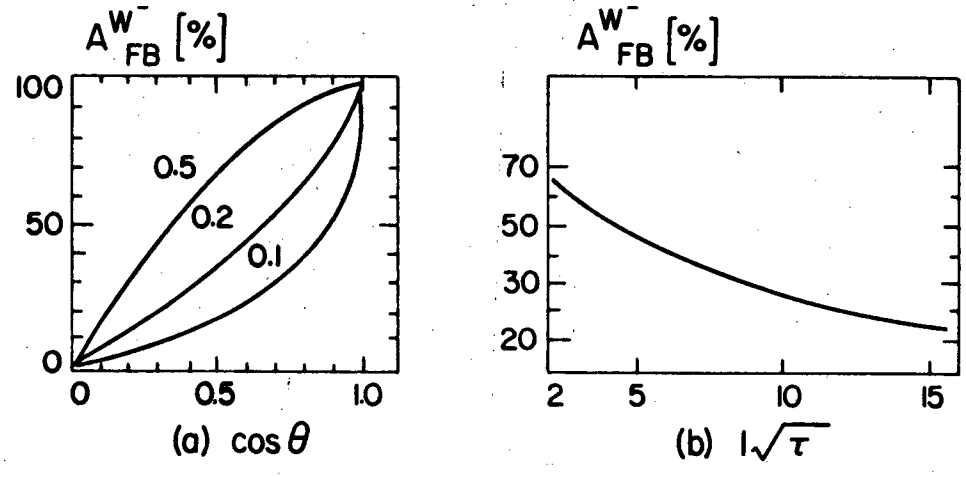

XBL 821-65

FIGURE 20

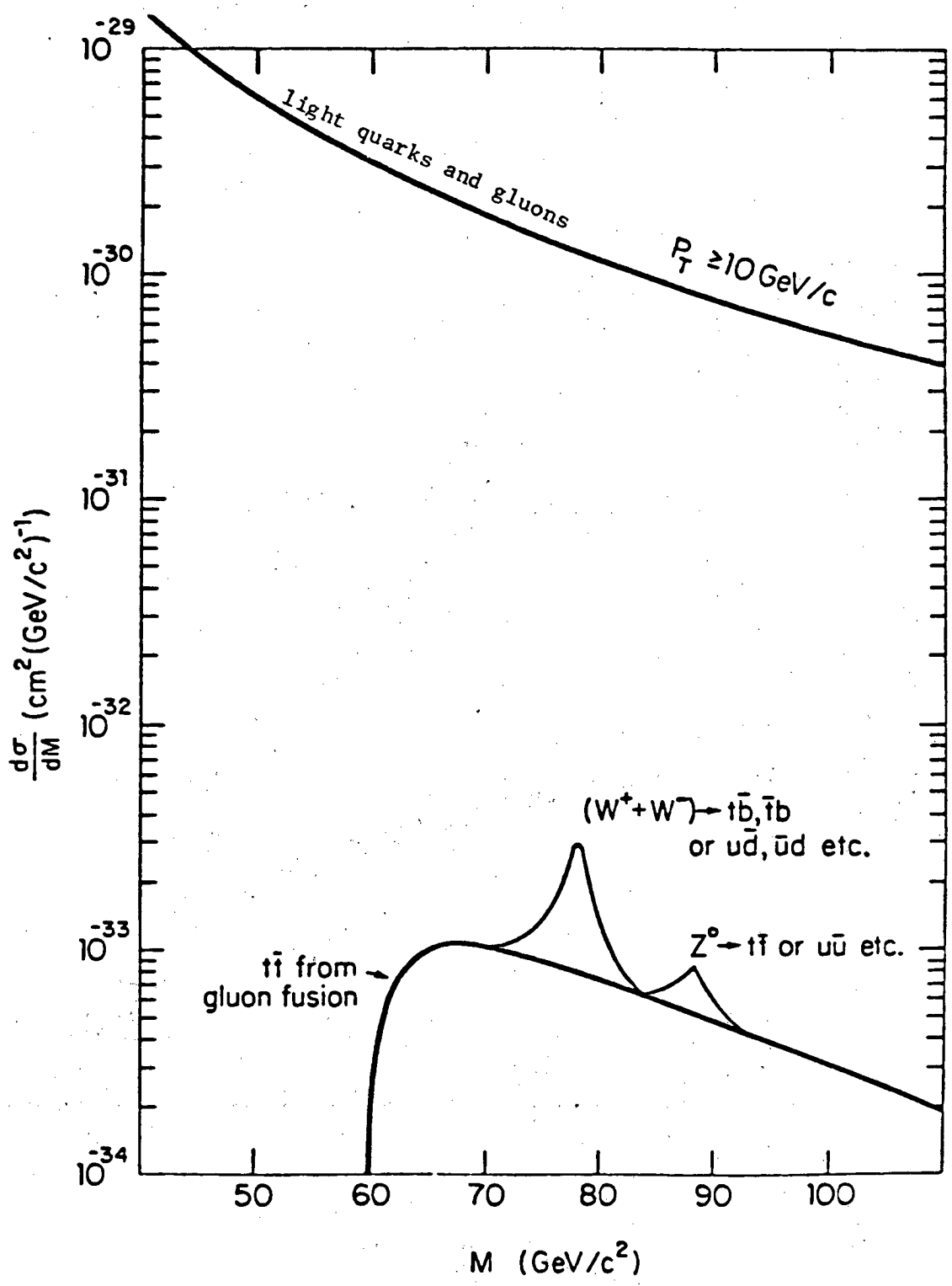
light quarks and gluons
$P_T \geq 10$ GeV/c
$(W^+ + W^-) \rightarrow t\bar{b}, \bar{t}b$
or $u\bar{d}, \bar{u}d$ etc.
$Z^\circ \rightarrow t\bar{t}$ or $u\bar{u}$ etc.
$t\bar{t}$ from
gluon fusion
$\frac{d\sigma}{dM}$ (cm^2(GeV/c^2)$^{-1}$)
10^{-29}
10^{-30}
10^{-31}
10^{-32}
10^{-33}
10^{-34}
50
60
70
80
90
100
M (GeV/c^2)

FIGURE 21

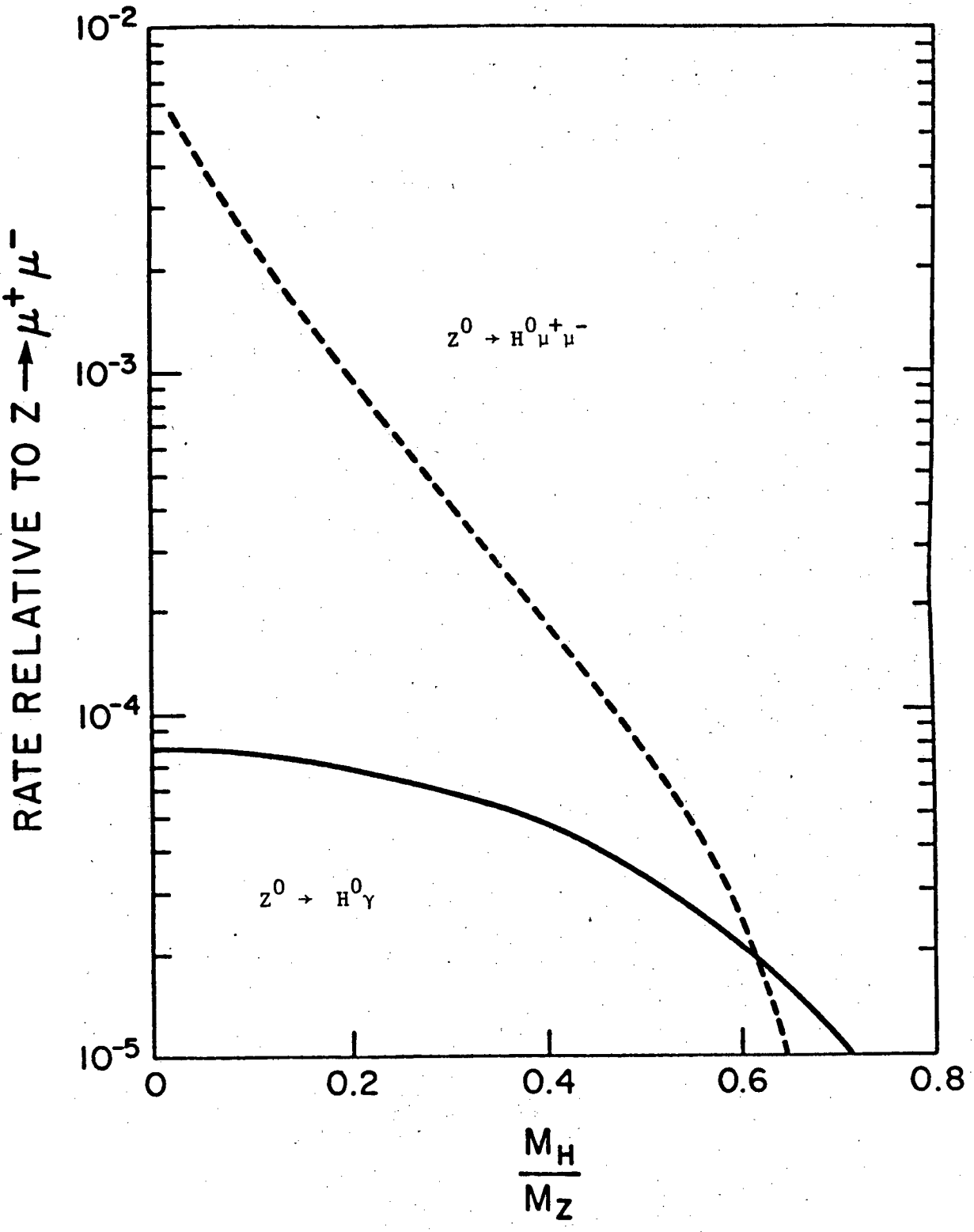
RATE RELATIVE TO Z→μ⁺μ⁻
10⁻²
10⁻³
10⁻⁴
10⁻⁵
Z⁰ → H⁰μ⁺μ⁻
Z⁰ → H⁰γ
0
0.2
0.4
0.6
0.8
M_H / M_Z

FIGURE 22

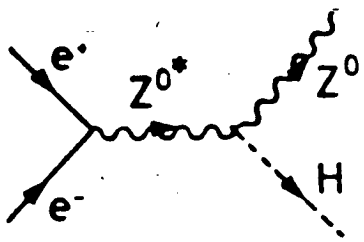

FIGURE 23

This report was done with support from the Department of Energy. Any conclusions or opinions expressed in this report represent solely those of the author(s) and not necessarily those of The Regents of the University of California, the Lawrence Berkeley Laboratory or the Department of Energy.

Reference to a company or product name does not imply approval or recommendation of the product by the University of California or the U.S. Department of Energy to the exclusion of others that may be suitable.

TECHNICAL INFORMATION DEPARTMENT
LAWRENCE BERKELEY LABORATORY
UNIVERSITY OF CALIFORNIA
BERKELEY, CALIFORNIA 94720